

A PRELIMINARY STUDY OF CONFIGURATION EFFECTS
ON THE DRAG OF A TRACTOR-TRAILER COMBINATION

By

THOMAS WACKER

B.A.Sc. (Mechanical Engineering), University of British Columbia, 1980

A THESIS SUBMITTED IN PARTIAL FULFILLMENT OF
THE REQUIREMENTS FOR THE DEGREE OF
MASTER OF APPLIED SCIENCE

in

THE FACULTY OF GRADUATE STUDIES
(Department of Mechanical Engineering)

We accept this thesis as conforming
to the required standard

THE UNIVERSITY OF BRITISH COLUMBIA

October, 1985

© Thomas Wacker, 1985

In presenting this thesis in partial fulfillment of the requirements for an advanced degree at the University of British Columbia, I agree that the library shall make it freely available for reference and study. I further agree that permission for extensive copying of this thesis for scholarly purposes may be granted by the Head of my Department or by his or her representatives. It is understood that copying or publication of this thesis for financial gain shall not be allowed without my written permission.

Thomas Wacker

Department of Mechanical Engineering
The University of British Columbia
2075 Wesbrook Place
Vancouver, Canada
V6T 1W5

Date: October, 1985

ABSTRACT

The effect of configuration changes and add-on devices on the drag reduction of a tractor-trailer is studied through wind tunnel tests using two 1/12-scale models. The configuration changes involve ground clearance, tractor-trailer gap, roof angle and back inclination while add-on devices include flow deflectors, skirts and gap seals. Moving surface boundary layer control as a means of drag reduction is also attempted. Both drag and pressure data are obtained to help identify local contributions. Results suggest that an optimum combination of configuration parameters can reduce drag up to 17% while the add-on devices resulted in a further decrease by a modest amount. The results with moving surface boundary layer control proved to be inconclusive.

TABLE OF CONTENTS

	<u>Page</u>
Abstract	ii
List of Tables	v
List of Figures	vi
List of Symbols	viii
Acknowledgement	ix
1. INTRODUCTION	1
1.1 Background	1
1.2 A Brief Review of Previous Work	1
1.3 Objectives	8
2. MODELS AND TEST PROCEDURES	9
2.1 Models	9
2.2 Add-on Devices	13
2.2.1 Tractor spoiler	13
2.2.2 Tractor roof deflector	13
2.2.3 Gap seals	13
2.3 Wind Tunnel	13
2.4 Wind Tunnel Balance	17
2.5 Instrumentation and Test Procedure	17

	<u>Page</u>
3. RESULTS AND DISCUSSION	19
3.1 Configuration Changes	19
3.1.1 Ground clearance and tractor-trailer gap	19
3.1.2 Trailer back angle	23
3.1.3 Trailer roof angle	28
3.1.4 Tractor roof angle	28
3.2 Reynolds Number Effects	32
3.3 Add-on Devices	32
3.3.1 Tractor spoiler	32
3.3.2 Tractor roof deflector	32
3.3.3 Gap seals	36
3.4 Moving Surface Boundary Layer Control	36
4. CONCLUDING REMARKS	42
4.1 Conclusions	42
4.2 Recommendations for Future Work	43
REFERENCES	44

LIST OF TABLES

	<u>Page</u>
3-1 Drag coefficient for various gap sealing configurations	38
3-2 Summary of drag reductions with various configurations and add-on devices	41

LIST OF FIGURES

	<u>Page</u>
1-1 Drag coefficient of several common bluff bodies, automobiles and a typical tractor-trailer configuration	2
1-2 A schematic diagram of Roshko and Koenig's [1] experimental set-up	3
1-3 Add-on devices used by Wong et al. [4]	5
1-4 Add-on devices and configuration changes used in the SAE study [6]	6
1-5 Correlation of fuel consumption and drag coefficient for full scale trucks as reported by Rose [7]	7
2-1 Photograph of the 1/12-scale model used in the configuration changes and add-on devices test program	10
2-2 A schematic diagram showing parameters studied during the configuration changes and add-on devices test program	11
2-3 Photograph of the 1/12-scale model used in the moving surface boundary layer control study	12
2-4 Photograph of the tractor spoiler	14
2-5 Photograph of the tractor roof deflector	15
2-6 A schematic diagram of the U.B.C. boundary layer wind tunnel	16
3-1 Drag coefficient versus ground clearance (H/L) for three different tractor-trailer gaps (G/L)	20
3-2 Variation of drag coefficient with tractor-trailer gap for a fixed ground clearance $H/L = 0.1$	21
3-3 Effect of ground clearance on drag coefficient for a fixed tractor-trailer gap $G/L = 0.1$	22
3-4 Typical pressure distribution on a conventional tractor-trailer configuration ($G/L = 0.1875$, $H/L = 0.0875$)	24
3-5 Pressure distribution on the optimum tractor-trailer configuration ($G/L = 0.1$, $H/L = 0.1$)	25
3-6 Drag coefficient versus trailer back angle θ	26

	<u>Page</u>
3-7 Pressure distribution on the optimum tractor-trailer configuration with 20° back angle	27
3-8 Variation of drag coefficient with trailer roof angle α for forward sloping roofs	29
3-9 Variation of drag coefficient with trailer roof angle α for backward sloping roofs	30
3-10 Effect of tractor roof angle β on drag coefficient	31
3-11 Variation of drag coefficient with Reynolds number for the optimum tractor-trailer configuration	33
3-12 Drag coefficient versus non-dimensional tractor spoiler width H_s/H_c	34
3-13 Variation of drag coefficient with tractor roof deflector angle γ for a given deflector length $C/L_c = 0.33$	35
3-14 Variation of drag coefficient with tractor roof deflector angle γ for a given deflector length $C/L_c = 0.5$	37
3-15 Effect of the trailer leading edge cylinder rotation on drag coefficient	39

LIST OF SYMBOLS

A	projected frontal area of model
C	tractor roof deflector length
C _d	drag coefficient, $D/(1/2\rho U^2 A)$
C _p	pressure coefficient, $(P-P_o)/(1/2\rho U^2)$
D	drag
G	tractor-trailer gap
H	trailer ground clearance
H _c	tractor height
H _s	spoiler width
L	trailer length
L _c	tractor roof length
P	pressure on model surface
P _o	static pressure
Re	Reynolds number, UL/ν
U	free stream velocity
V	rotating cylinder surface velocity
α	trailer roof angle
β	tractor roof angle
γ	tractor roof deflector angle
θ	trailer back angle
ν	air viscosity
ρ	air density

ACKNOWLEDGEMENT

This study was supported by the Natural Sciences and Engineering Research Council of Canada, Grant No. A-2181.

Thanks go to Mr. Ed Abell for construction of the wind tunnel models and to Mr. Andrew Kwok for his help with the wind tunnel tests.

A special thank you is extended to Dr. V. J. Modi for his time and guidance throughout the project and to my wife, Meg, for her patience and encouragement.

1. INTRODUCTION

1.1 Background

With the ever rising price of fuel, it has become increasingly important to reduce road vehicle fuel consumption. As a substantial portion of goods in Canada are transported by trucks, even a small reduction in aerodynamic drag (and hence fuel consumption) can result in a significant yearly saving in transportation costs.

Since trucks function as bulk load carriers, they necessarily have a large frontal area. Frontal area cannot be significantly reduced due to length and height constraints, hence a reduction in the drag coefficient becomes the only practical method of minimizing the aerodynamic resistance.

It would be useful at this point to compare the drag of a typical tractor-trailer configuration to that of some common bluff bodies and automobiles. Figure 1-1 shows such a comparison.

1.2 A Brief Review of Previous Work

Given the importance of this topic, there has obviously been much research done.

At a fundamental level, Roshko and Koenig [1] studied the interaction between two bluff bodies placed in tandem. A disk was located upstream of a flat faced cylinder over a range of gap sizes and the forebody drag measured. Figure 1-2 shows a simplified layout of the model used. In the optimum configuration ($d_1/d_2 = 0.75$, $g/d_2 = 0.375$) a drag reduction of 97% with reference to the cylinder alone was observed.

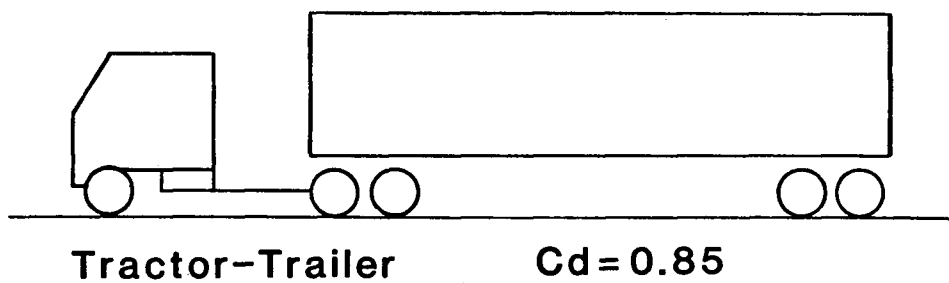
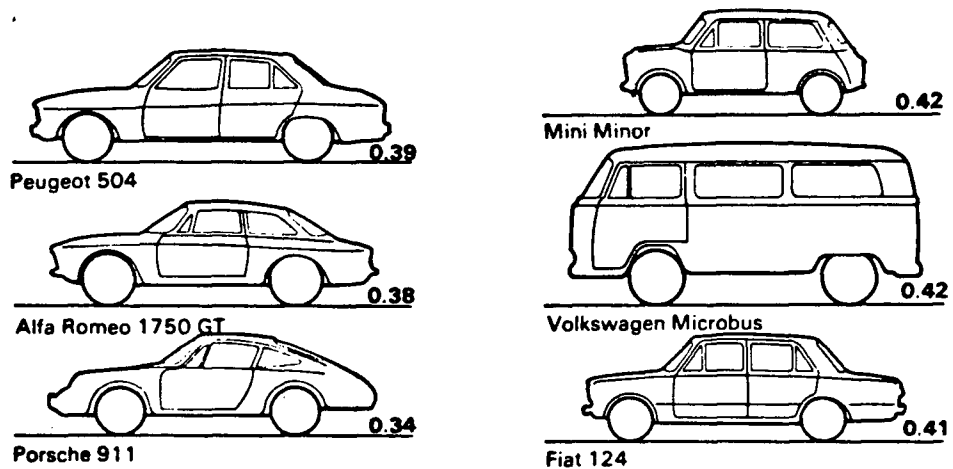
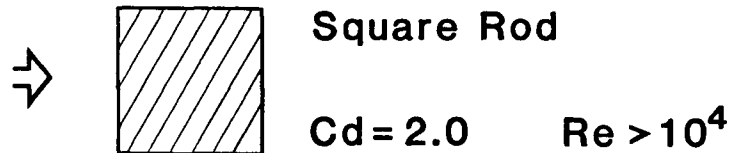
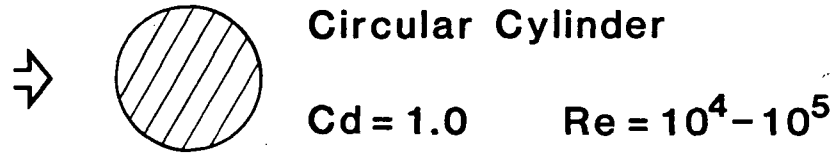


Figure 1-1. Drag coefficient of several common bluff bodies, automobiles and a typical tractor-trailer configuration.

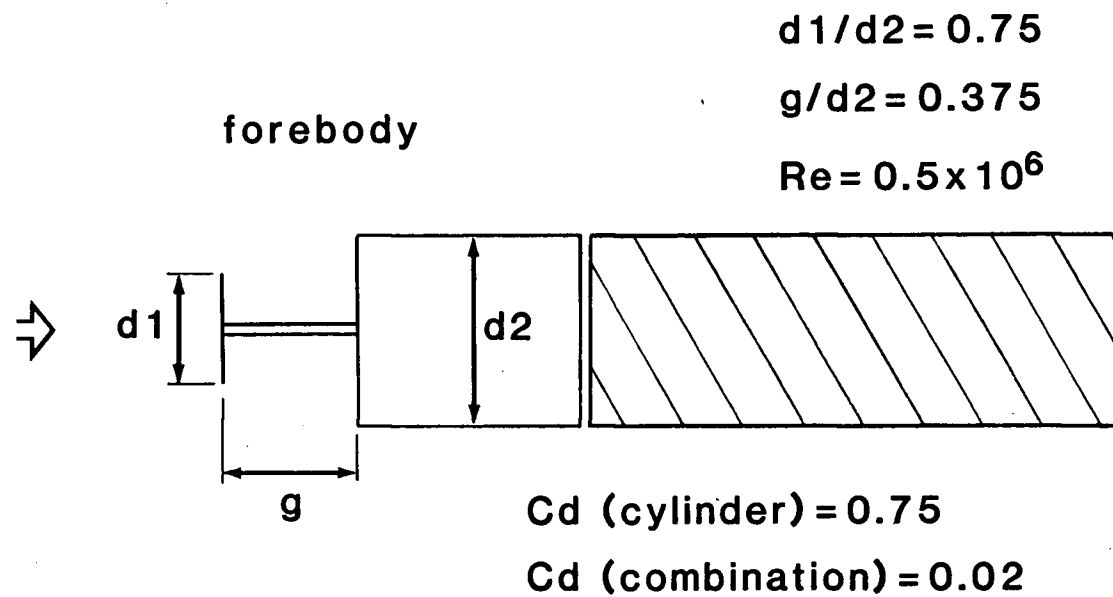


Figure 1-2. A schematic diagram of Roshko and Koenig's [1] experimental set-up.

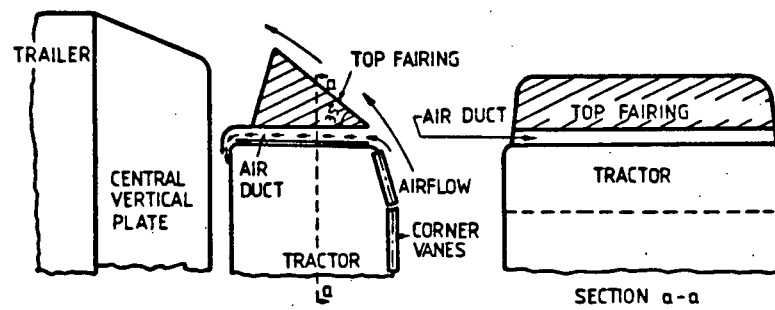
The results are later compared to those obtained in the present study with tractor-trailer separation.

In essentially qualitative studies, Ahmed and Baumert [2], and Mair [3] examined flow patterns behind road vehicles and axi-symmetric bodies with various rear end shapes. The object was to reduce the wake and hence the drag. Similar ideas are explored in this work.

Wong et al. [4], Mason and Beebe [5] and a study sponsored by the Society of Automotive Engineers [6] have conducted wind tunnel tests on tractor-trailer models. Wong et al., using a 1/18-scale model, reported a 28% drag reduction with the configuration shown in Figure 1-3. Mason and Beebe tested several 1/7-scale models and reported a 34% drag reduction using a roof fairing alone. The SAE study involved 1/8-scale models with several add-on devices. Figure 1-4 shows the different configurations tested. A maximum drag reduction of 34% was obtained using a combination of roof fairing and trailer corner rounding.

Full scale tests using add-on devices were conducted by Rose [7]. Drag reductions were then correlated with fuel savings. Figure 1-5 shows these results. The highest measured drag reduction of 36% corresponded to a 16% reduction in fuel consumption.

In the field of boundary layer control, Modi et al. [8] studied the effects of momentum injection on the performance of an airfoil while Catalano et al. [9] attempted to reduce the wake of a road vehicle by introduction of unsteady vortex shedding into the flow field at the rear of the vehicle. Both the studies showed quite promising results and possible application of the concept to tractor-trailer combinations.



$C_d \text{ (base)} = 0.93$

$C_d \text{ (optimum)} = 0.674$

Figure 1-3. Add-on devices used by Wong et al. [4].

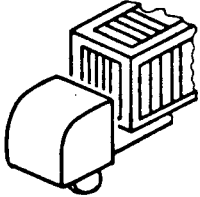
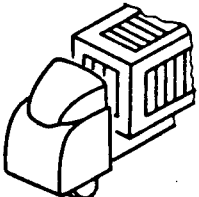
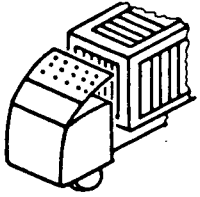
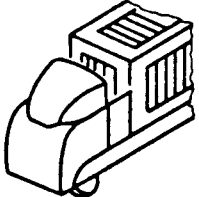
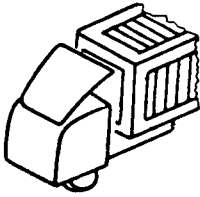
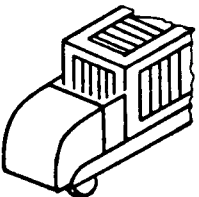
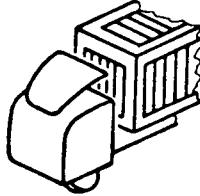
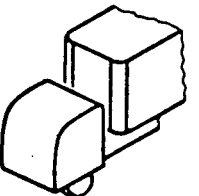
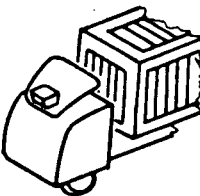
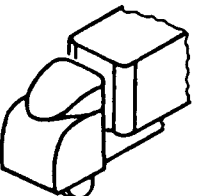
	C_D	C_D Reduction %		C_D	C_D Reduction %
	0.863	—		0.656	24
	0.663	23.2		0.629	27.1
	0.660	23.5		0.820	4.2
	0.657	23.8		0.673	22
	0.668	22.6		0.568	34.1

Figure 1-4. Add-on devices and configuration changes used in the SAE study [6].

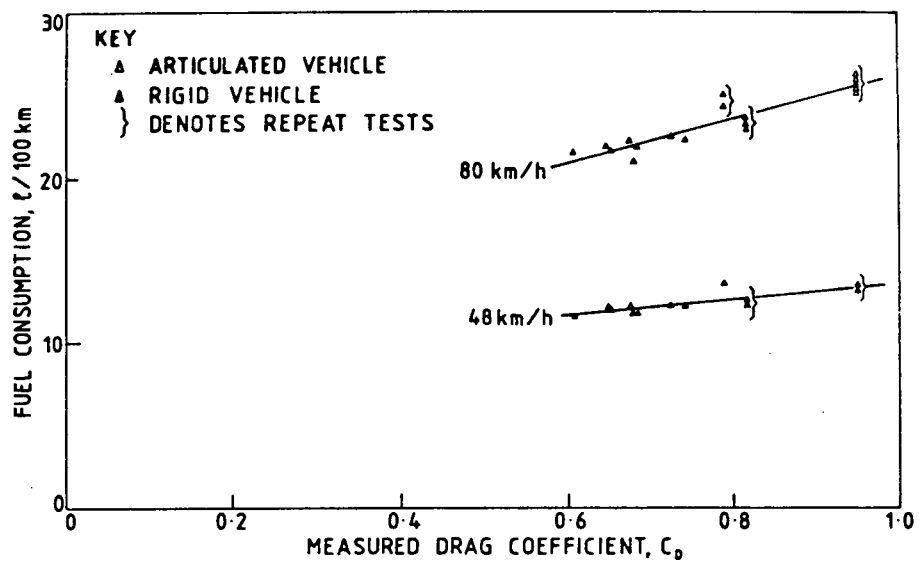


Figure 1-5. Correlation of fuel consumption and drag coefficient for full scale trucks as reported by Rose [7].

1.3 Objectives

The objectives of this study are fourfold: (i) None of the previous investigators have attempted to arrive at an optimum base configuration of a tractor-trailer, i.e., the combination of ground clearance and tractor-trailer gap producing the least drag. (ii) One cannot accurately compare the results of previous investigations with add-on devices since they were used on different base configurations. In the present study the effectiveness of add-on devices is assessed using the same base configuration to get an accurate estimate of their performance. (iii) The study explores the feasibility of using moving surface boundary layer control to reduce the drag of road vehicles. (iv) Results obtained by different investigators using different models (size and geometrical details), test facilities (tunnel boundary layer, turbulence intensity, blockage) and conditions (Reynolds number) seldom compare due to complex corrections involved. The main objective of this test program is to provide a sound database through a systematic study with configuration changes and add-on devices using the same model and test conditions.

2. MODELS AND TEST PROCEDURES

2.1 Models

Two 1/12-scale Plexiglas models were used in the wind tunnel tests. Both were somewhat idealized, lacking wheels, detailed undersides and other minor components (mirrors, exhaust stacks, etc.). The models were fitted with pressure taps to give some appreciation as to the local contribution to the overall drag.

The first model (Figure 2-1) was used in tests with various add-on devices and with different tractor-trailer configurations. This model was constructed in modular form, to permit the use of different trailer roofs and backs. Ground clearance and tractor-trailer gap could also be varied. Figure 2-2 shows the various parameters studied during the test program.

The second model (Figure 2-3) was used during the boundary layer control study. Cylinders were mounted at the leading and trailing edges of the tractor and trailer roofs. Each cylinder was driven by an internally mounted D.C. motor, allowing for individual rotational speed control. Power was transmitted via an o-ring friction drive. For this model, ground clearance and tractor-trailer gap were fixed at the optimum values found in tests with the first model.

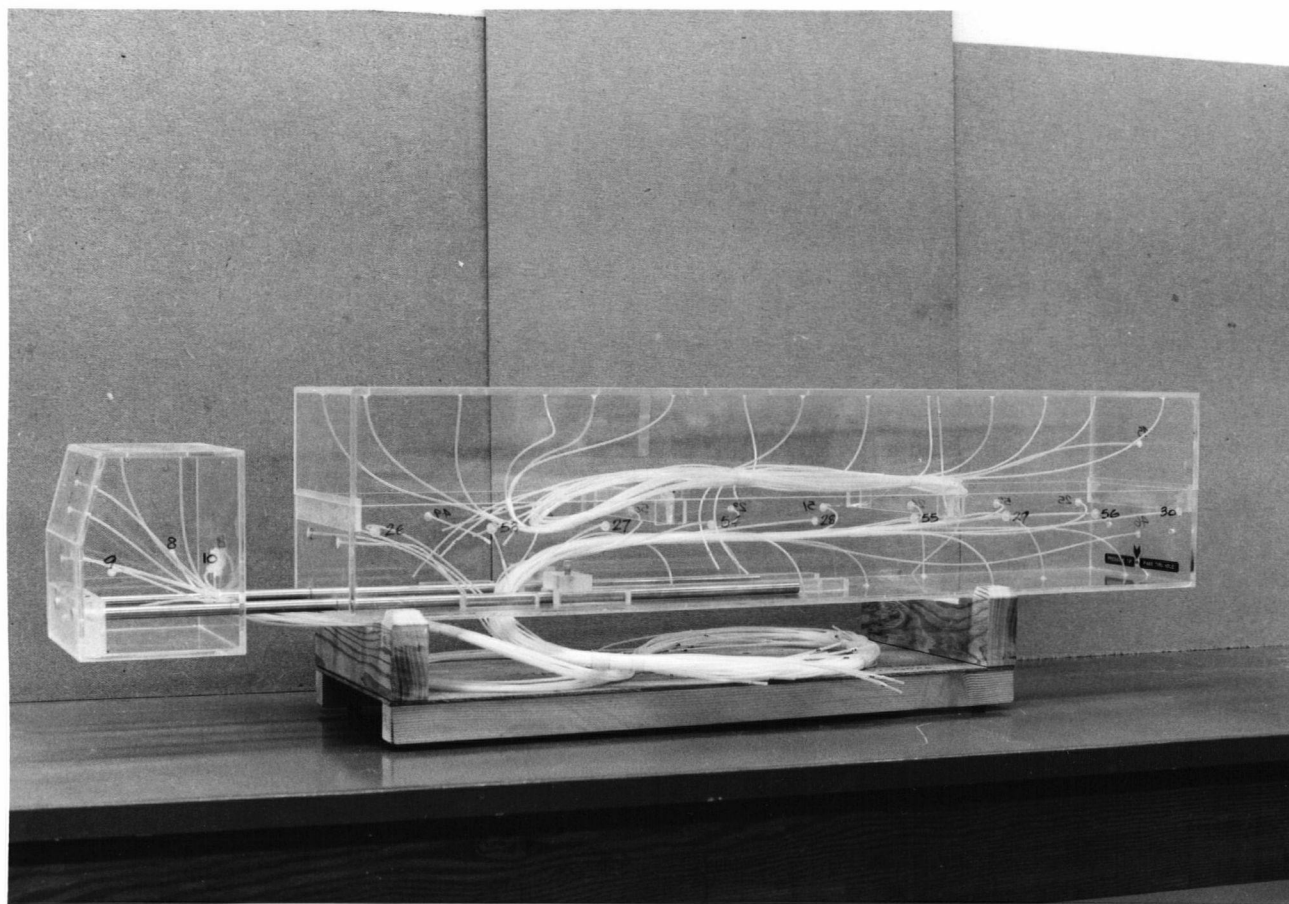


Figure 2-1. Photograph of the 1/12-scale model used in the configuration changes and add-on devices test program

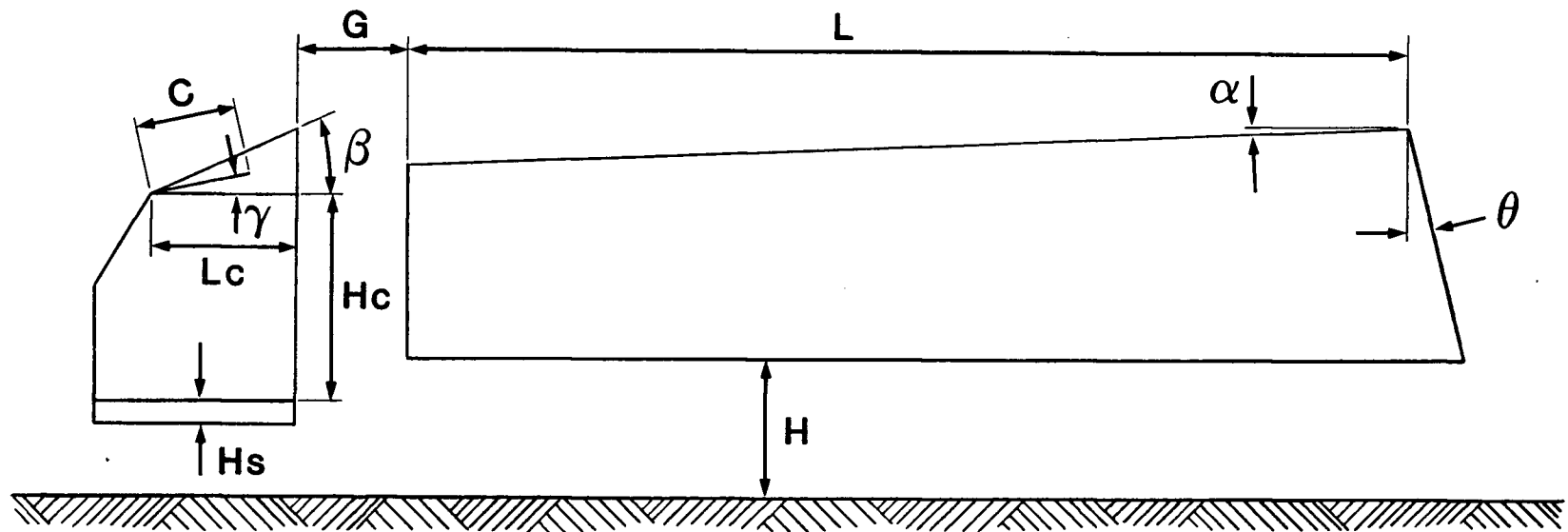


Figure 2-2. A schematic diagram showing parameters studied during the configuration changes and add-on devices test program

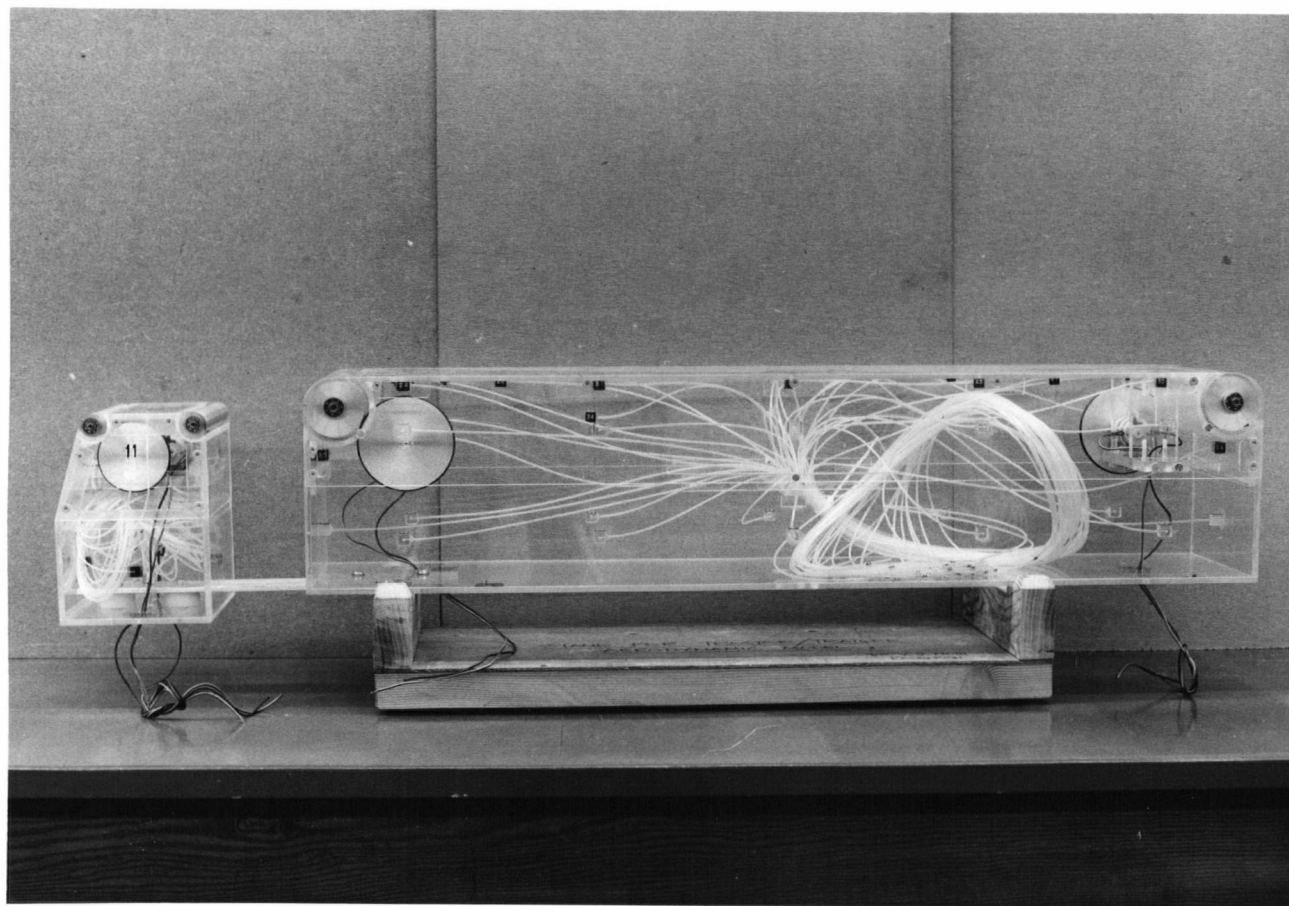


Figure 2-3. Photograph of the 1/12-scale model used in the moving surface boundary layer control study

2.2 Add-on Devices

2.2.1 Tractor spoiler

This device (Figure 2-4) consists of a front airdam and side skirts attached to the bottom of the tractor. The skirts extend the full length of the tractor. Three spoiler widths (H_s) were tested: 2.5 cm, 3.8 cm and 5.1 cm.

2.2.2 Tractor roof deflector

The deflector (Figure 2-5) consists of a flat plate attached to the front edge of the tractor roof and extending its full width. Tests were conducted with deflector lengths (C) of 4.5 cm and 6.75 cm at various angles of inclination (γ).

2.2.3 Gap seals

The gap seals are in the form of flat plates extending from the back-edge of the tractor roof, sides or bottom to the corresponding front edge of the trailer. The seals were tested alone and in combinations. The side seals were always tested together.

2.3 Wind Tunnel

The tests were conducted in the U.B.C. boundary layer wind tunnel (Figure 2-6). The tunnel is an open-circuit type powered by an 80 kW three phase motor which drives an axial flow fan at a constant 700 rpm. Velocity is varied using a pneumatic controller to alter the blade pitch. Velocity range is 2.5 to 25 m/s with an undisturbed turbulence

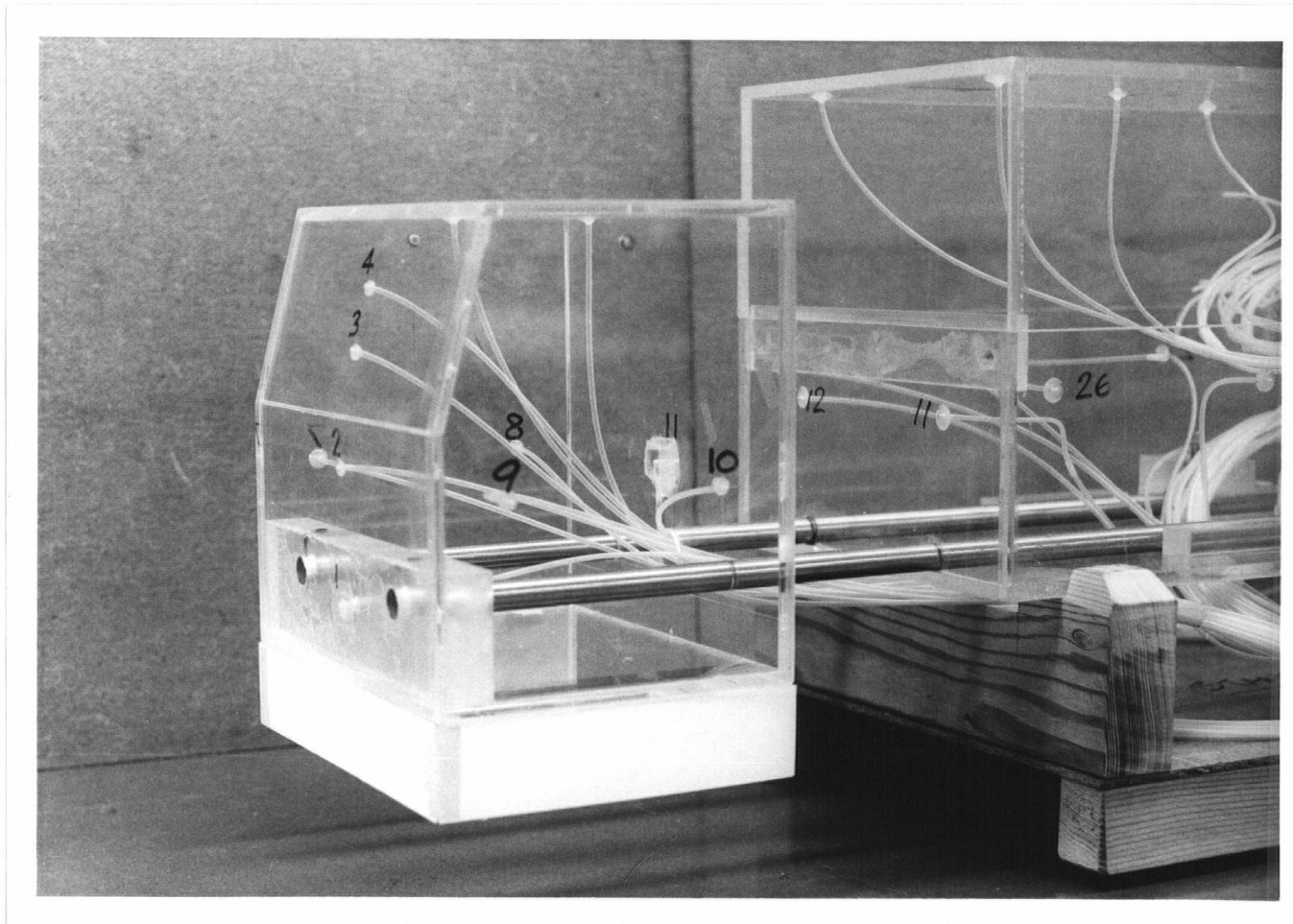


Figure 2-4. Photograph of the tractor spoiler

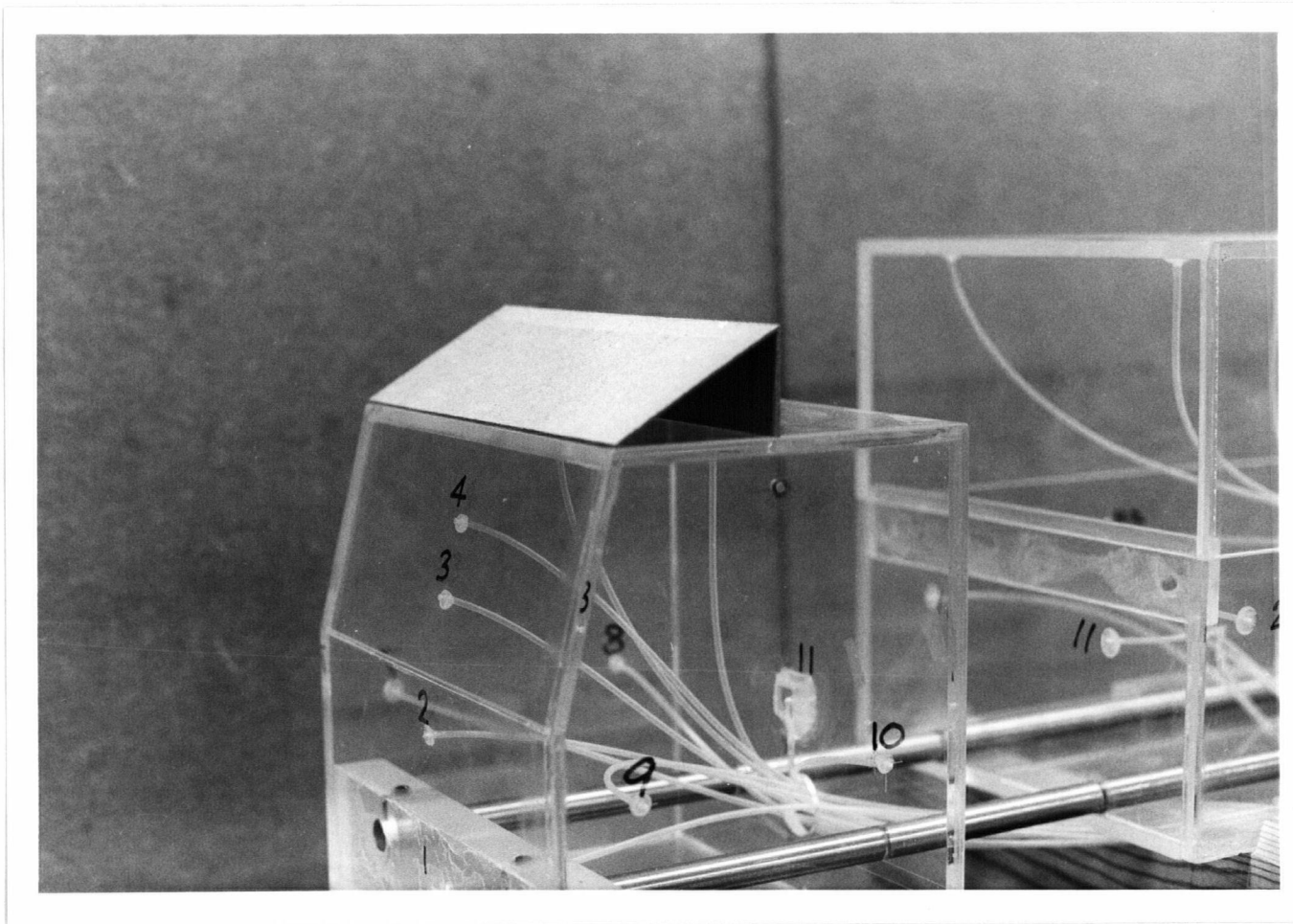


Figure 2-5. Photograph of the tractor roof deflector

Axivane Series 2000 Rotor,

2.44 m dia.,

16 Cast aluminum blades,

80 kW electric motor,

175,000 cfm at 700 rpm,

Fisher 480-60 pneumatic
variable pitch control

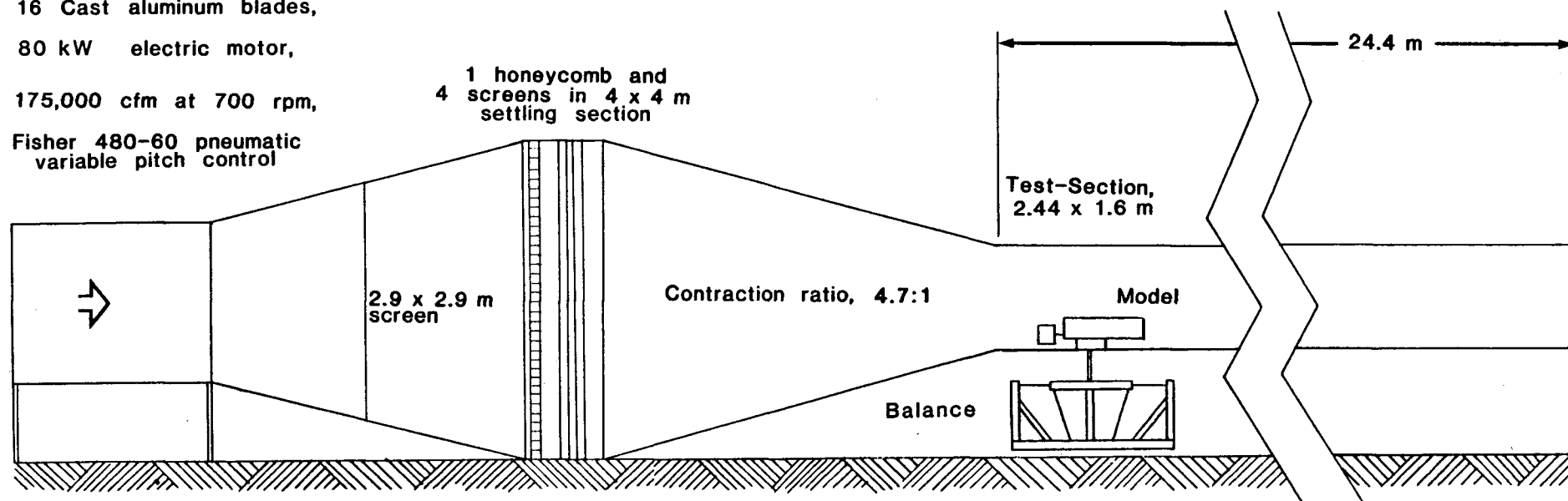


Figure 2-6. A schematic diagram of the U.B.C. boundary layer wind tunnel

level of less than 1%. Spatial variation of mean velocity in the test section is less than 2%.

The settling section contains a honeycomb and four screens to smooth the flow as it enters a 4.7 to 1 contraction which accelerates the flow and improves its uniformity. The test section is 24.4 m long with a cross section of 2.44 m x 1.62 m at its entrance. The adjustable test section roof was set for a zero pressure gradient.

2.4 Wind Tunnel Balance

Force measurements were carried out using an Aerolab strain gauge balance. It is capable of measuring the three principal forces and moments acting on a model. During a typical test, only drag was recorded, although side force was monitored to ensure alignment with the tunnel axis (zero yaw angle).

2.5 Instrumentation and Test Procedure

Balance signals were amplified and read with a digital voltmeter. The amplifier was calibrated so that the reading in volts corresponded to the drag in pounds-force.

Wind tunnel dynamic head was measured with a pitot static tube connected to a Lambrecht manometer. Atmospheric pressure and wind tunnel temperature were also recorded to translate the dynamic head into velocity.

Due to the small area ratio ($A_{\text{model}}/A_{\text{tunnel}} = 0.014$), drag readings were not corrected for blockage effects.

To compensate for drift in the balance signal amplifier, the

following test procedure was used. An initial 'drag' reading was taken with the tunnel on but at zero velocity. The tunnel velocity was then set to the desired value and a drag reading noted once the flow was stabilized. The tunnel was then returned to zero velocity and a final 'drag' reading taken. As an additional check, the clean configuration (no add-on devices) drag was measured at the beginning and the end of each series of tests.

3. RESULTS AND DISCUSSION

3.1 Configuration Changes

3.1.1 Ground clearance and tractor-trailer gap

Figure 3-1 shows the variation of drag coefficient versus non-dimensional ground clearance (H/L) for three different non-dimensional gaps: $G/L = 0.0875$, 0.1 and 0.1125 . Reynolds number was 0.64×10^6 for all the tests. These results established the optimum (i.e., minimum drag) base configuration on which all subsequent modifications were based. All three curves show the same trend with minimum drag occurring at approximately the same ground clearance of $H/L = 0.1$. The tests with $G/L = 0.1$ resulted in the lowest drag value of $C_d = 0.668$. This then established the optimum combination of gap and ground clearance at $G/L = 0.1$ and $H/L = 0.1$.

It should be pointed out here that a typical configuration found on today's tractor-trailers is $G/L = 0.1875$ and $H/L = 0.0875$. Testing this configuration resulted in a drag coefficient of $C_d = 0.71$.

To illustrate the above results in clearer terms, the two parameters were varied separately. Figure 3-2 shows the effects of varying gap with ground clearance fixed at $H/L = 0.1$ and Figure 3-3 shows the effects of varying ground clearance with gap fixed at $G/L = 0.1$.

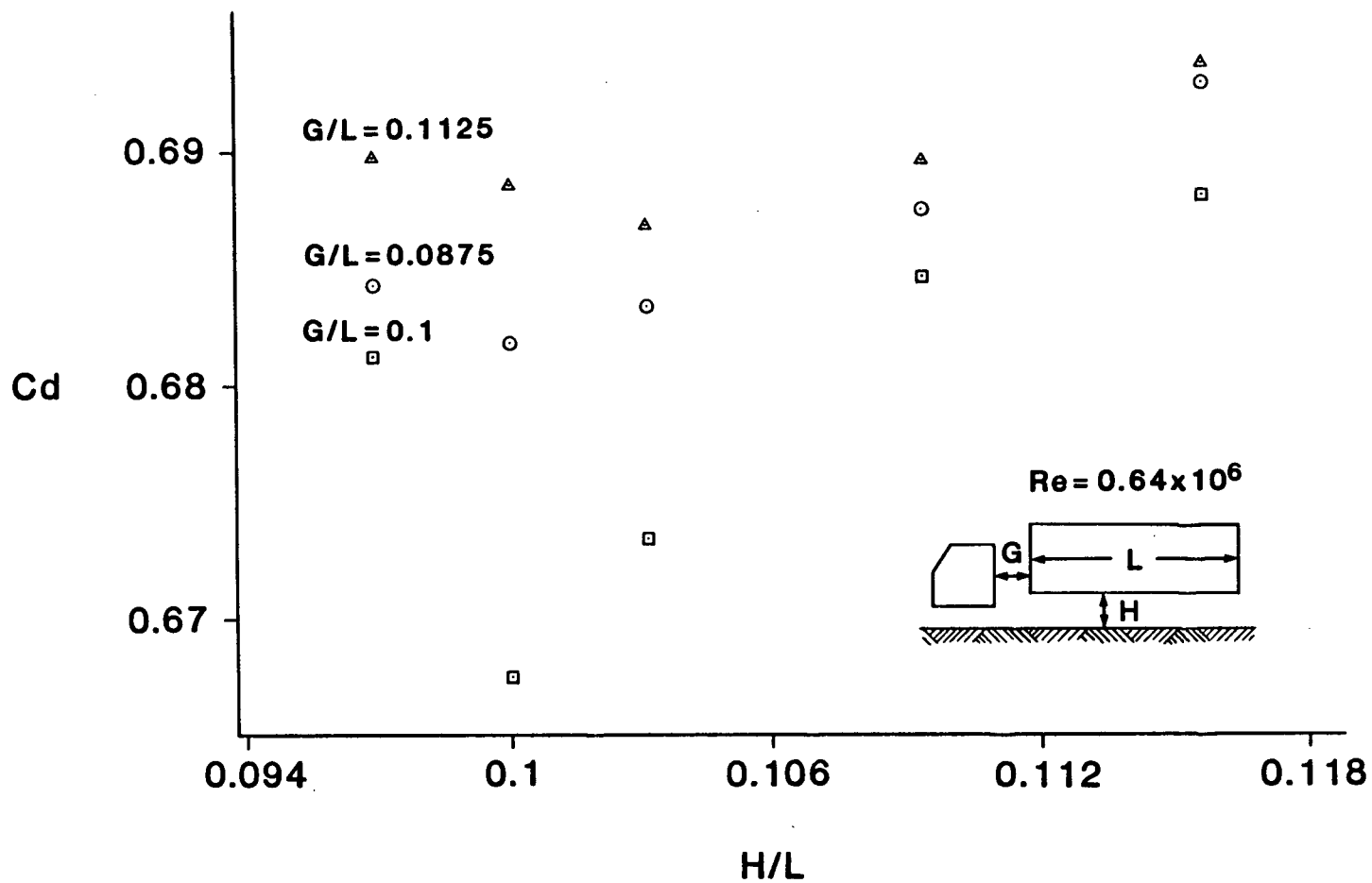


Figure 3-1. Drag coefficient versus ground clearance (H/L) for three different tractor-trailer gaps (G/L)

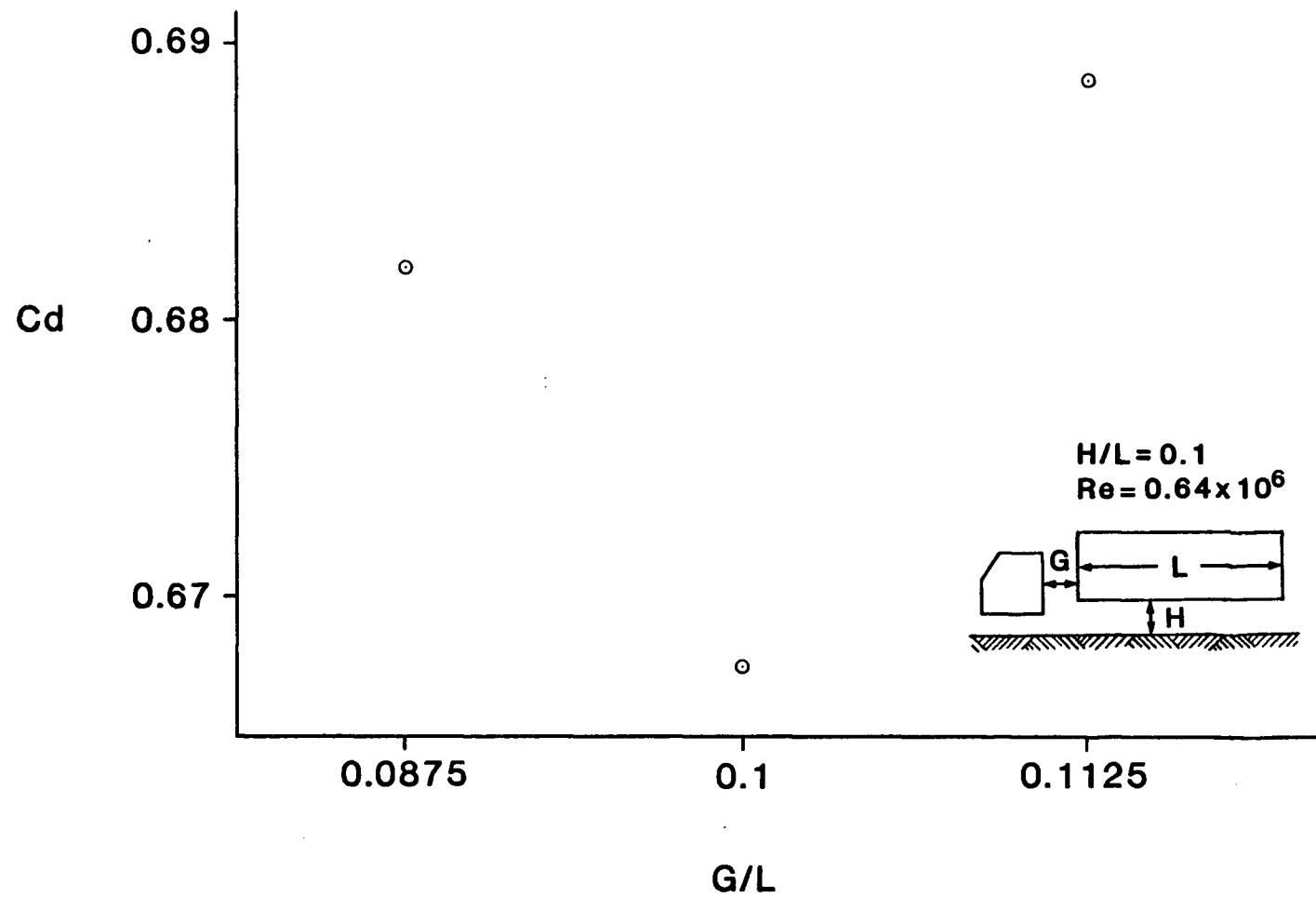


Figure 3-2. Variation of drag coefficient with tractor-trailer gap for a fixed ground clearance $H/L = 0.1$

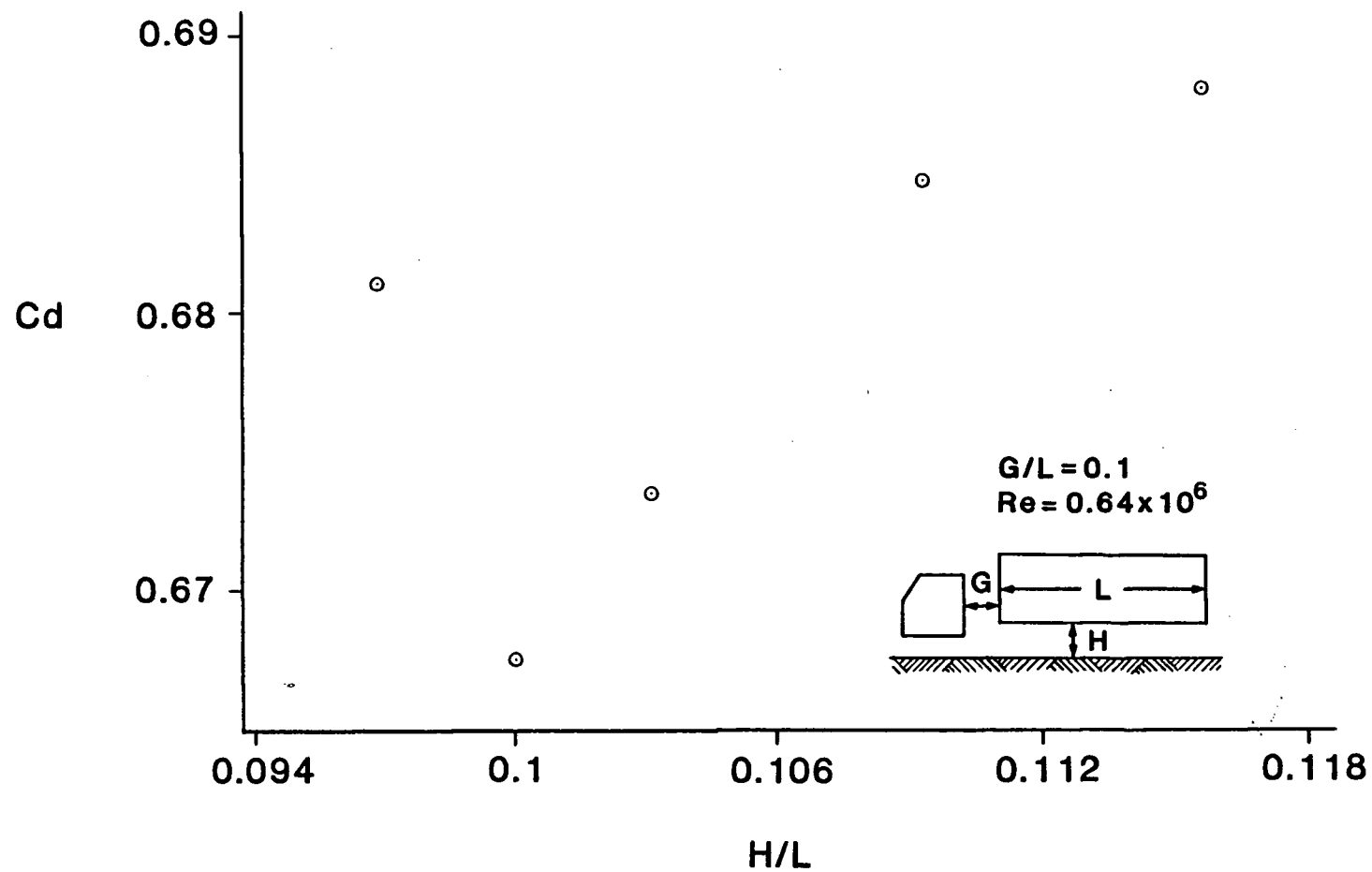


Figure 3-3. Effect of ground clearance on drag coefficient for a fixed tractor-trailer gap $G/L = 0.1$

To obtain better appreciation as to the local contribution to the drag, pressure distributions were measured on the conventional ($G/L = 0.1875$, $H/L = 0.0875$) and optimum ($G/L = 0.1$, $H/L = 0.1$) configurations. The results are shown in Figures 3-4 and 3-5. The major difference between the two is a larger negative pressure region at the rear of the conventional configuration. This is clearly a contributing factor leading to a higher drag.

3.1.2 Trailer back angle

With optimum gap and ground clearance established, other configuration parameters could now be varied to explore the possibility of further reduction in drag. Figure 3-6 shows the variation of drag coefficient with the trailer back angle (θ) at a Reynolds number of 0.64×10^6 . Minimum drag was observed at an angle of 20° with a very sharp increase at angles above 30° . The decrease in drag from 0° to 20° is attributed to the flow being able to negotiate the shallower angle at the top edge. The increase in drag at higher angles is presumably due to separation from the sides and bottom edge.

To verify the mechanism of drag reduction, a pressure distribution was charted with $\theta = 20^\circ$. Figure 3-7 clearly shows a smaller rear separation bubble compared to the base configuration shown in Figure 3-5.

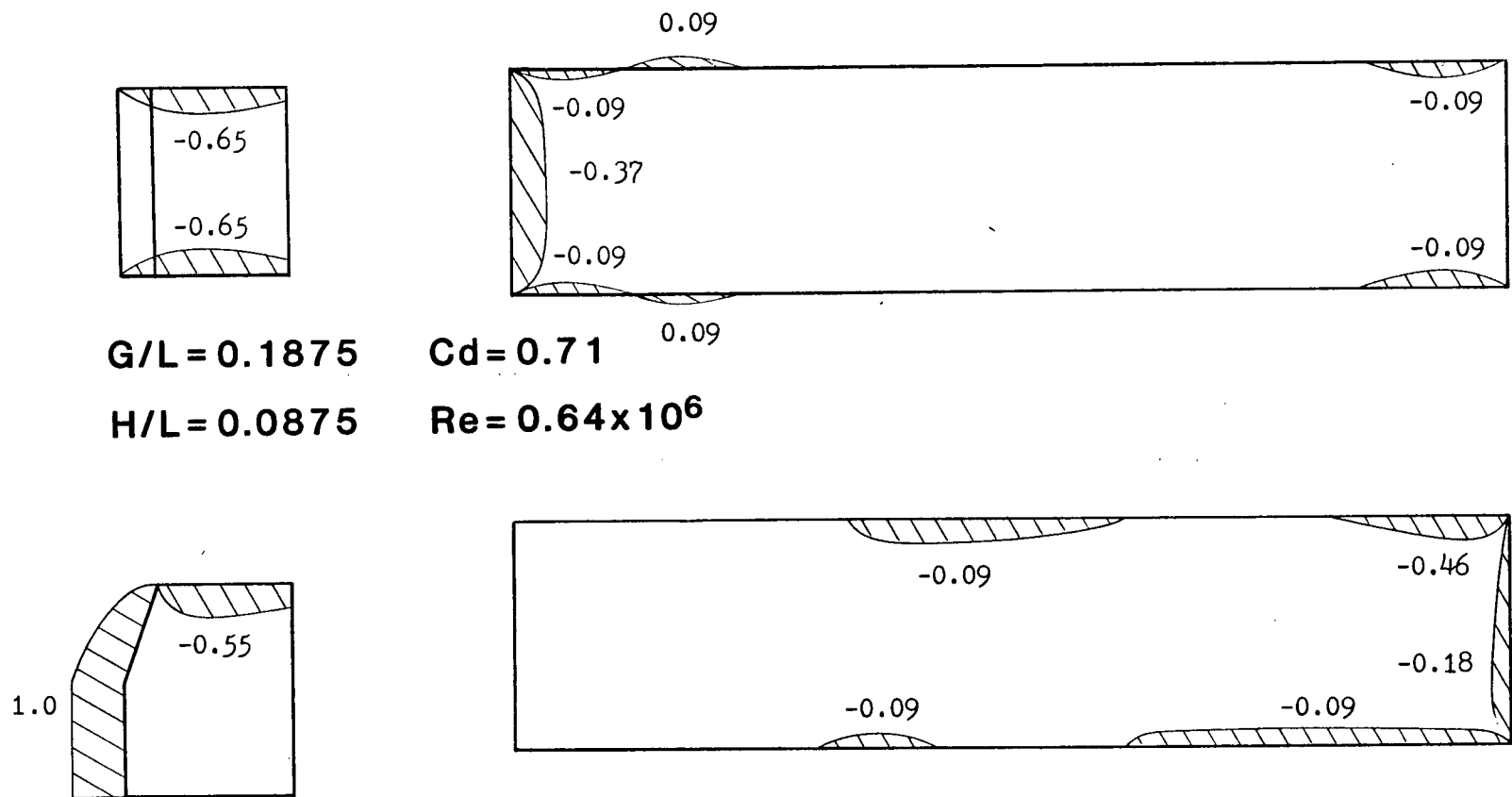


Figure 3-4. Typical pressure distribution on a conventional tractor-trailer configuration ($G/L = 0.1875$, $H/L = 0.0875$)

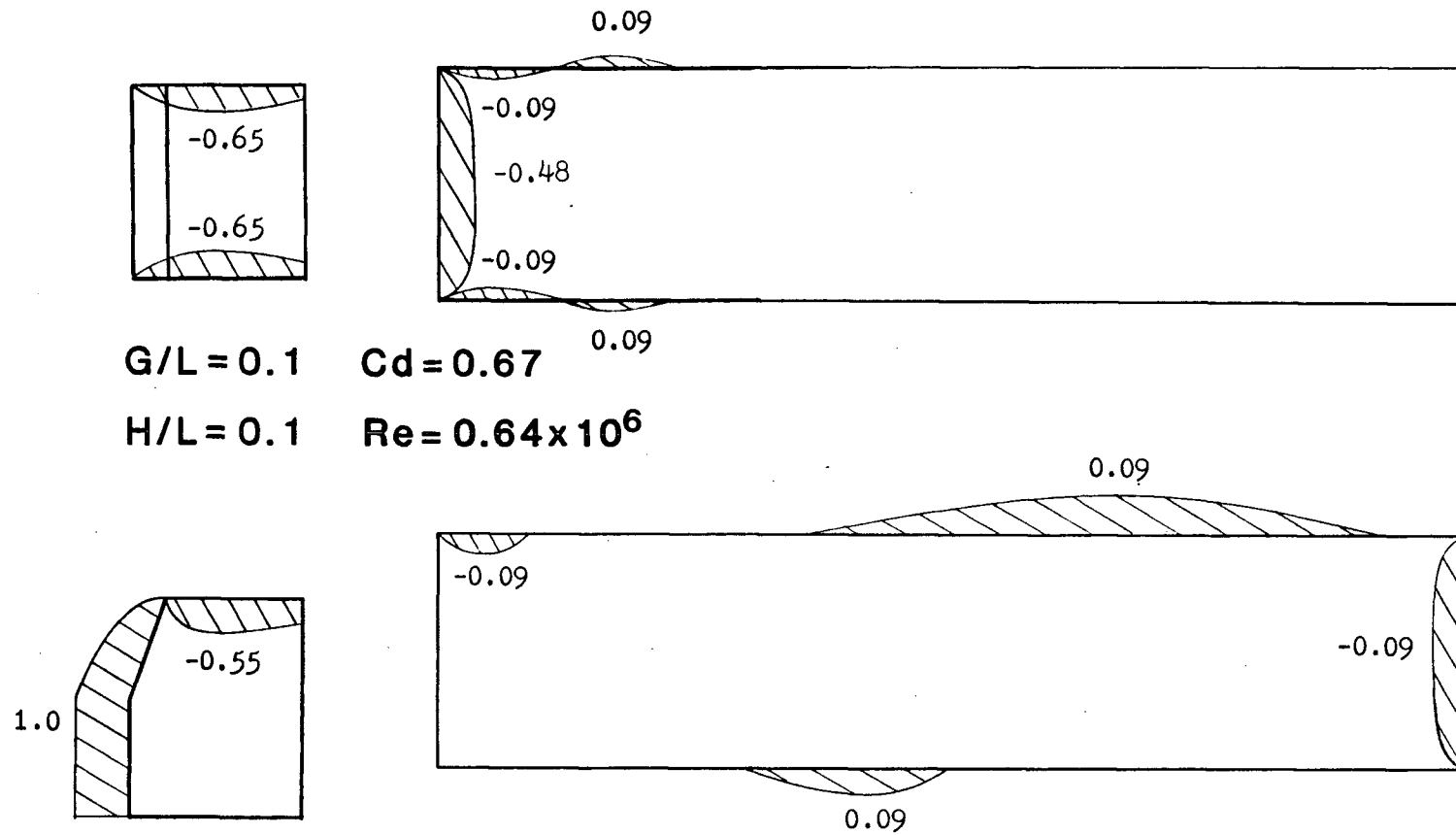


Figure 3-5. Pressure distribution on the optimum tractor-trailer configuration ($G/L = 0.1$, $H/L = 0.1$)

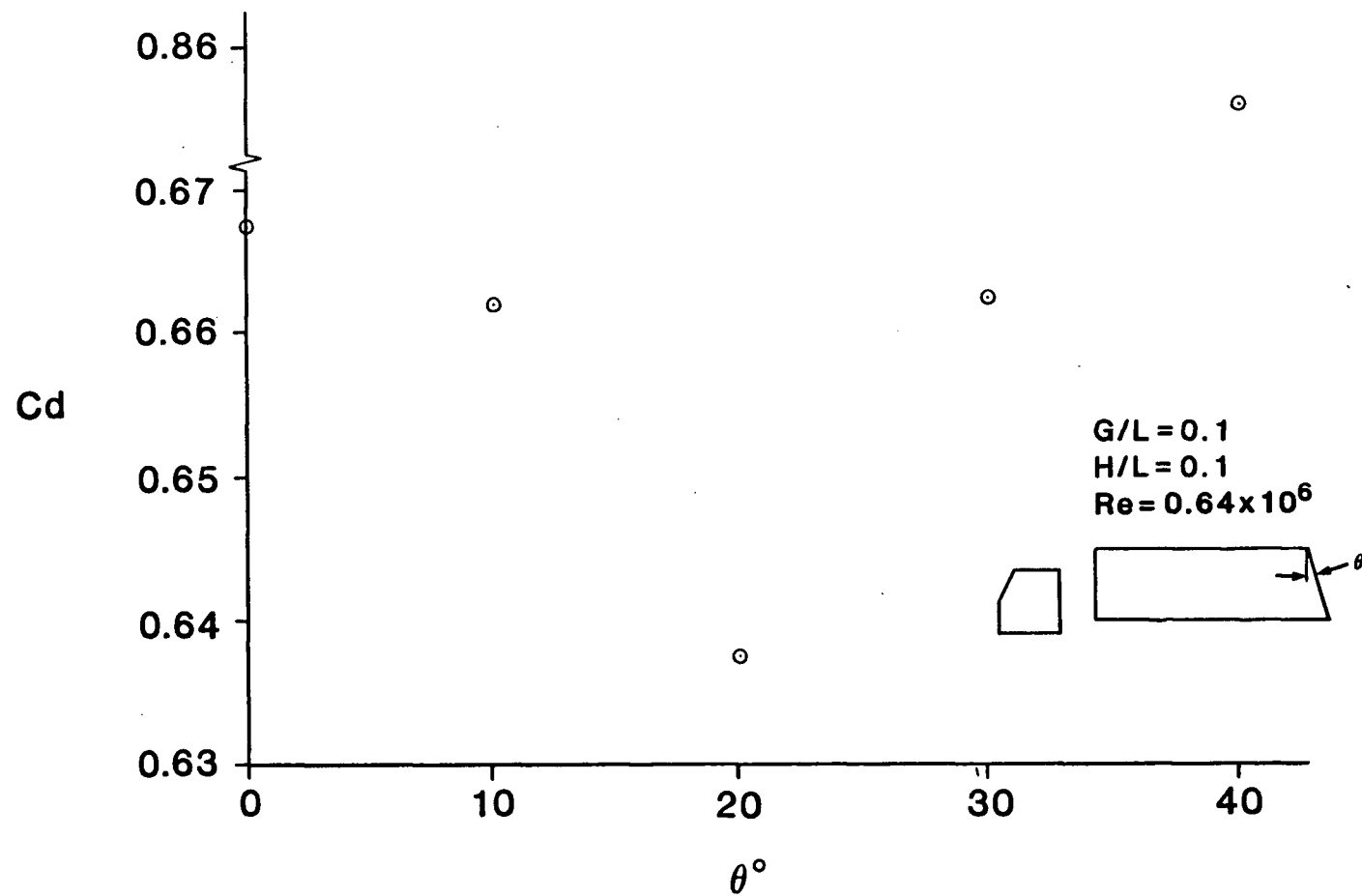


Figure 3-6. Drag coefficient versus trailer back angle θ

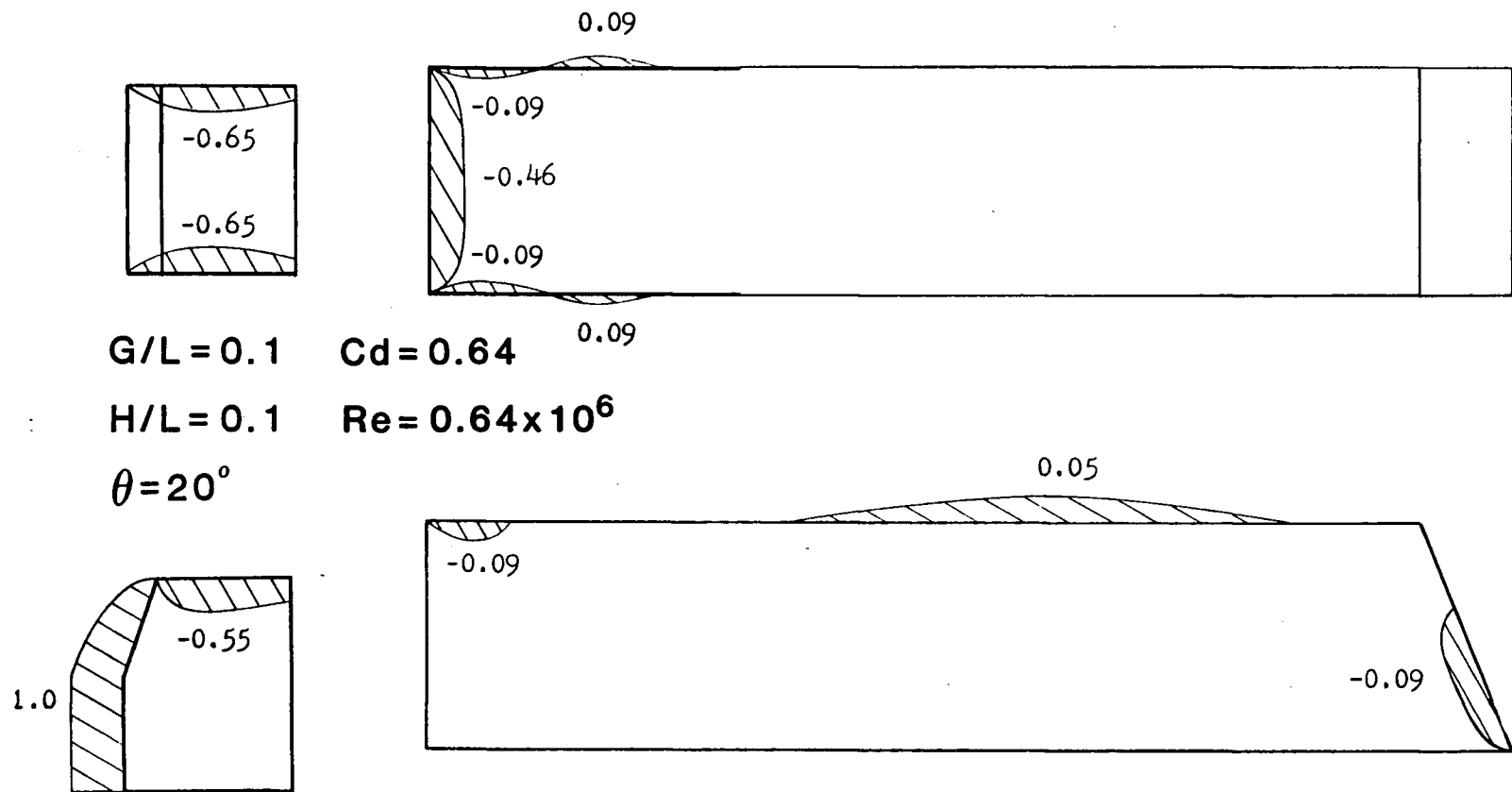


Figure 3-7. Pressure distribution on the optimum tractor-trailer configuration with 20° back angle

3.1.3 Trailer roof angle

Two sets of tests were run with a variable trailer roof angle, α . Figure 3-8 shows drag coefficient versus α for forward sloping roofs at a Reynolds number of 0.59×10^6 . Corresponding results for backward sloping roofs are presented in Figure 3-9. The forward sloping roofs show a steady increase in angle while the trend is reversed for backward sloping roofs. This is explained by the fact that for backward sloping roofs, the flow encounters a shallower angle at the back while for forward sloping roofs, the angles become greater with increasing roof slope. There could also be more favourable gap geometry with backward sloping roofs although this would require a further study to verify.

3.1.4 Tractor roof angle

Figure 3-10 shows the variation of drag coefficient with tractor roof angle (β) at a Reynolds number of 0.56×10^6 . Although the drag is always greater than the base value ($\beta = 0^\circ$), there is a considerable dip in the curve at $\beta = 20^\circ$. This would imply that 20° is close to the angle required for smooth reattachment of the flow to the front of the trailer. Other inclinations resulted in a larger separation bubble and hence a higher drag coefficient.

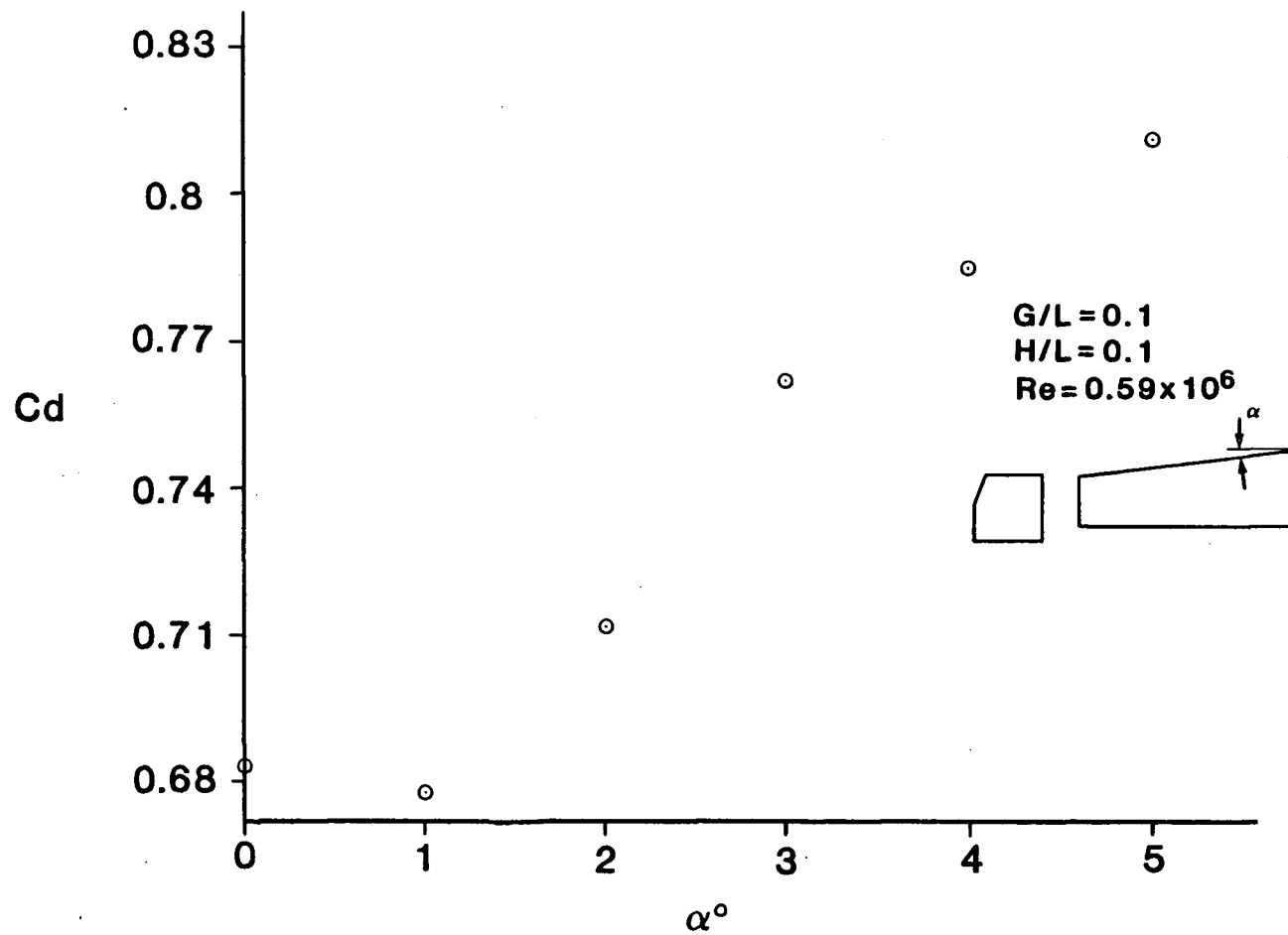


Figure 3-8. Variation of drag coefficient with trailer roof angle α for forward sloping roofs

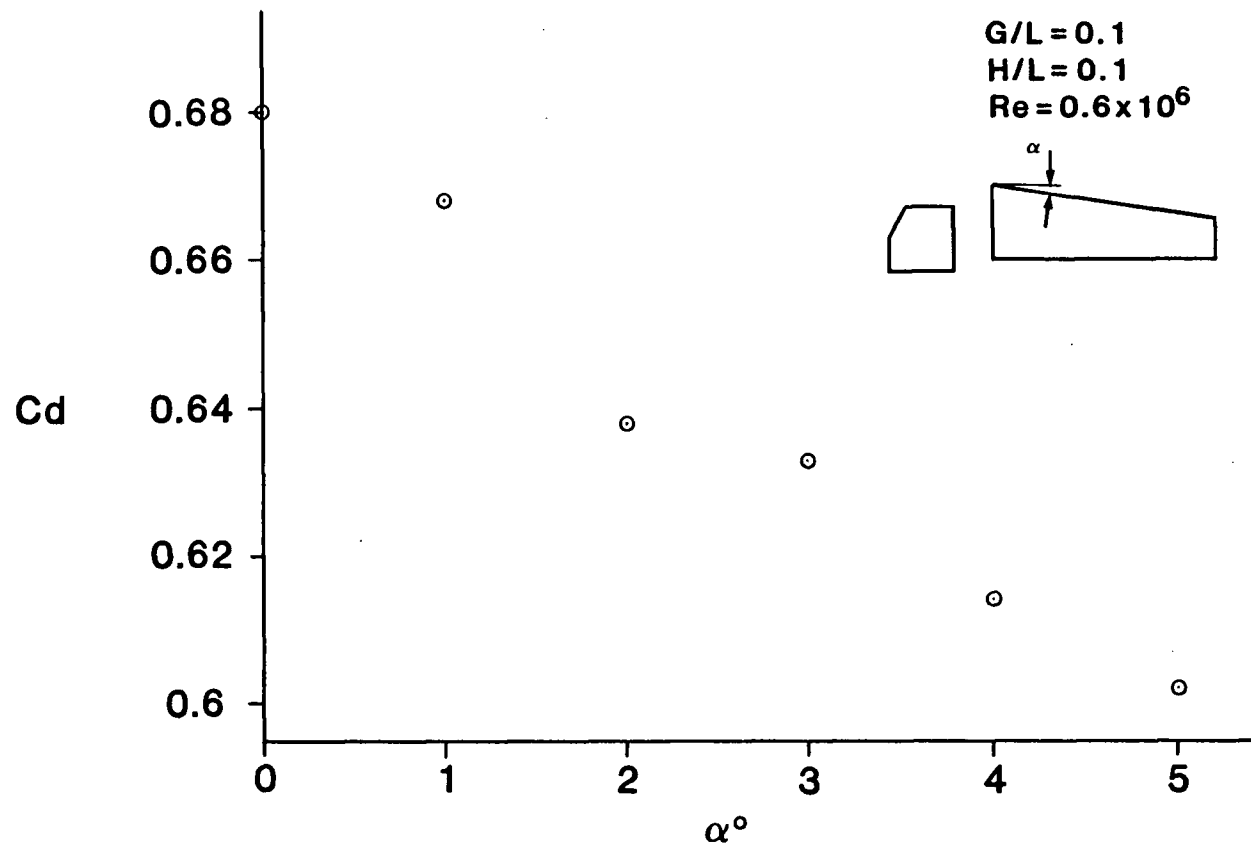


Figure 3-9. Variation of drag coefficient with trailer roof angle α for backward sloping roofs

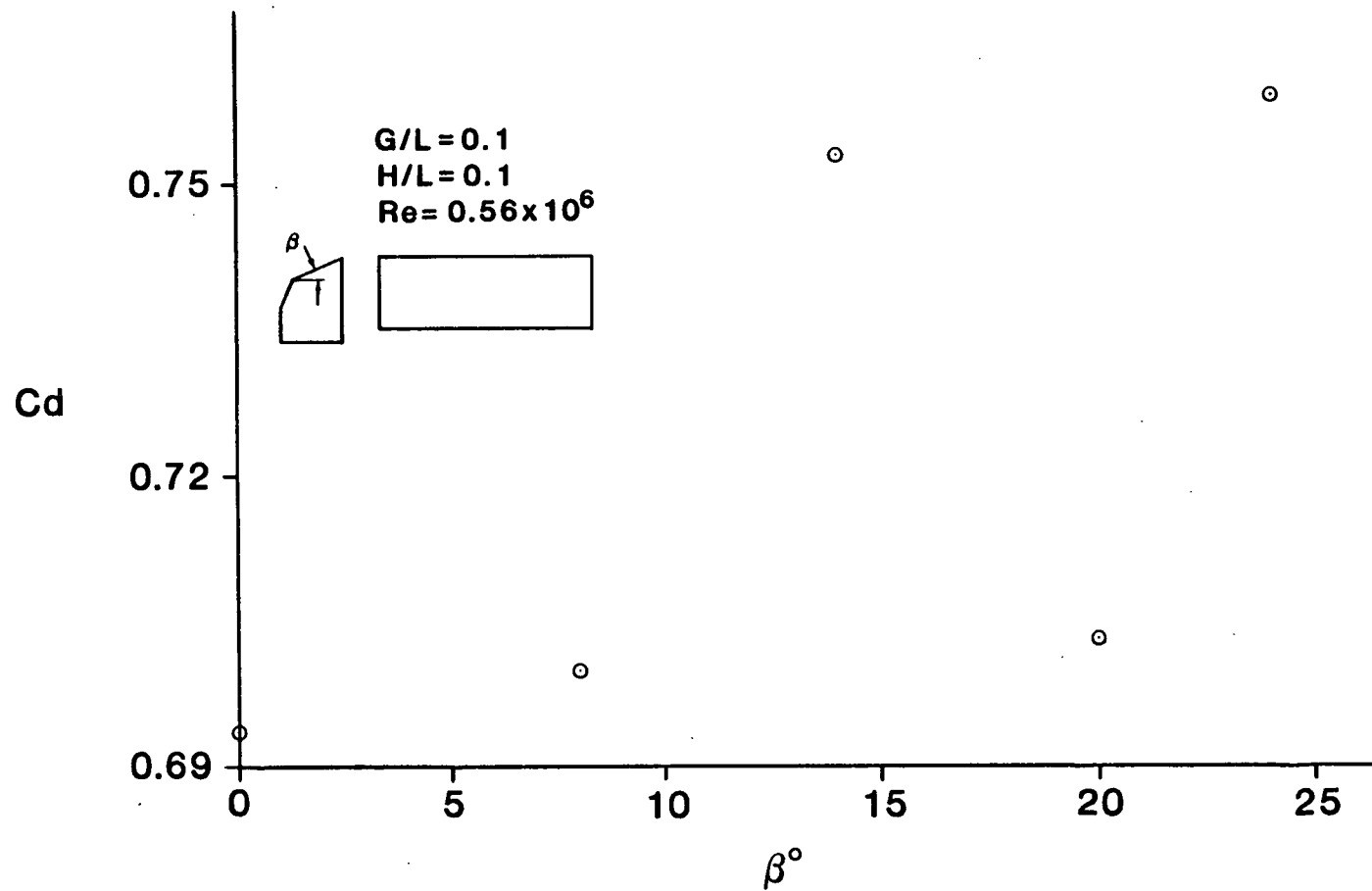


Figure 3-10. Effect of tractor roof angle β on drag coefficient

3.2 Reynolds Number Effects

Preliminary tests suggested drag of the base configuration ($G/L = 0.1$, $H/L = 0.1$) to be dependent on the Reynolds number. To establish the dependence more precisely a systematic study was undertaken. Figure 3-11 shows the results.

A steady decrease in drag coefficient with increasing Reynolds number is apparent. This is in agreement with the results of the configuration tests.

3.3 Add-on Devices

3.3.1 Tractor spoiler

Figure 3-12 shows drag coefficient versus non-dimensional spoiler width (H_s/H_c) at a Reynolds number of 0.56×10^6 . A steady increase in drag with an increase in spoiler width is observed. For a model with a detailed underside, this trend would be, probably, reversed as the spoiler reduces the separated flow on the underside. With a smooth underside, however, the effect of adding a spoiler is the same as reducing the ground clearance, which results in an increase in drag.

3.3.2 Tractor roof deflector

The tractor roof deflector tests were conducted for two deflector lengths, C/L_c . Figure 3-13 shows variation of the drag coefficient with deflector angle (γ) for $C/L_c = 0.33$ at a Reynolds number of 0.568×10^6 , while Figure 3-14 presents results for C/L_c

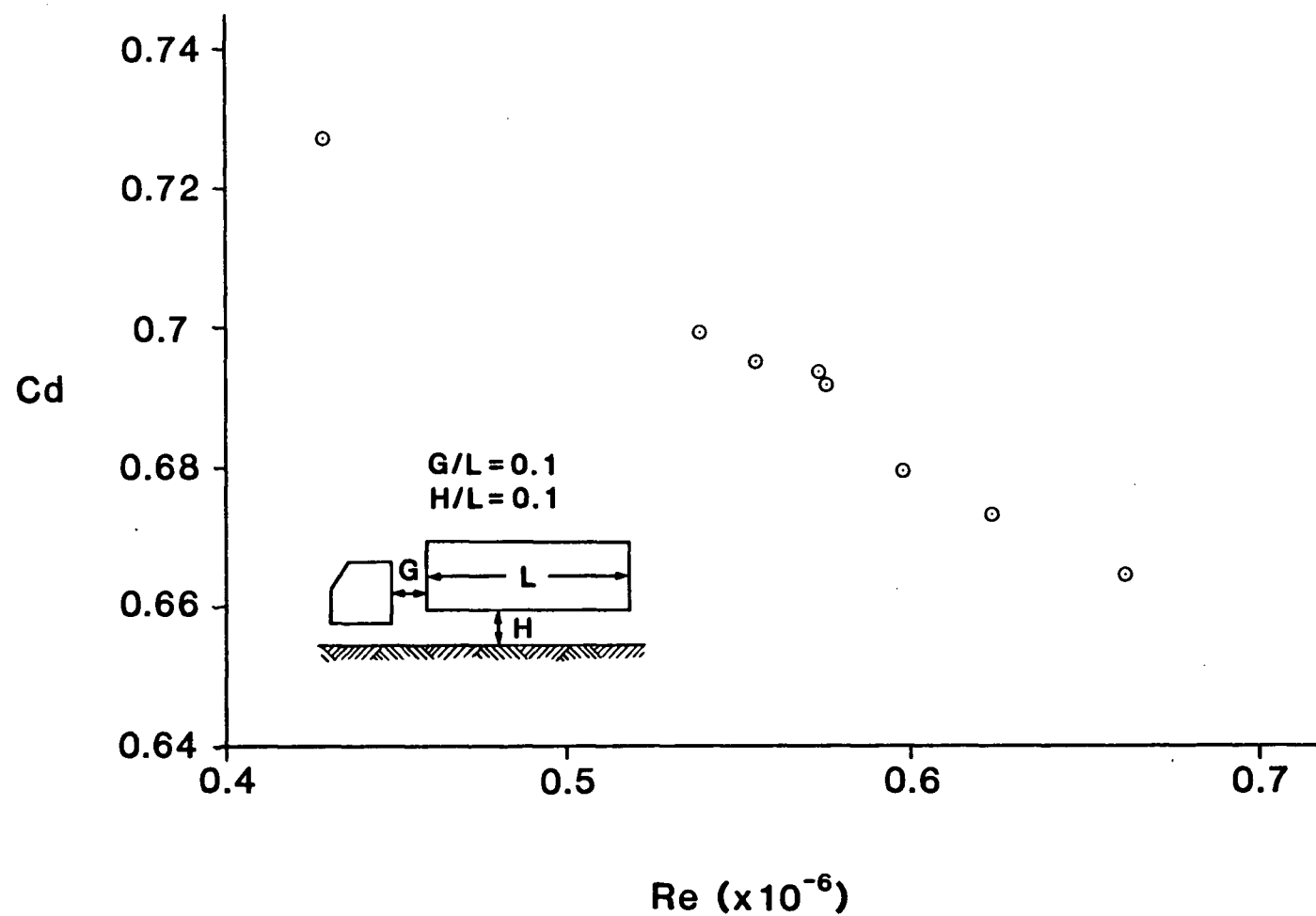


Figure 3-11. Variation of drag coefficient with Reynolds number for the optimum tractor-trailer configuration

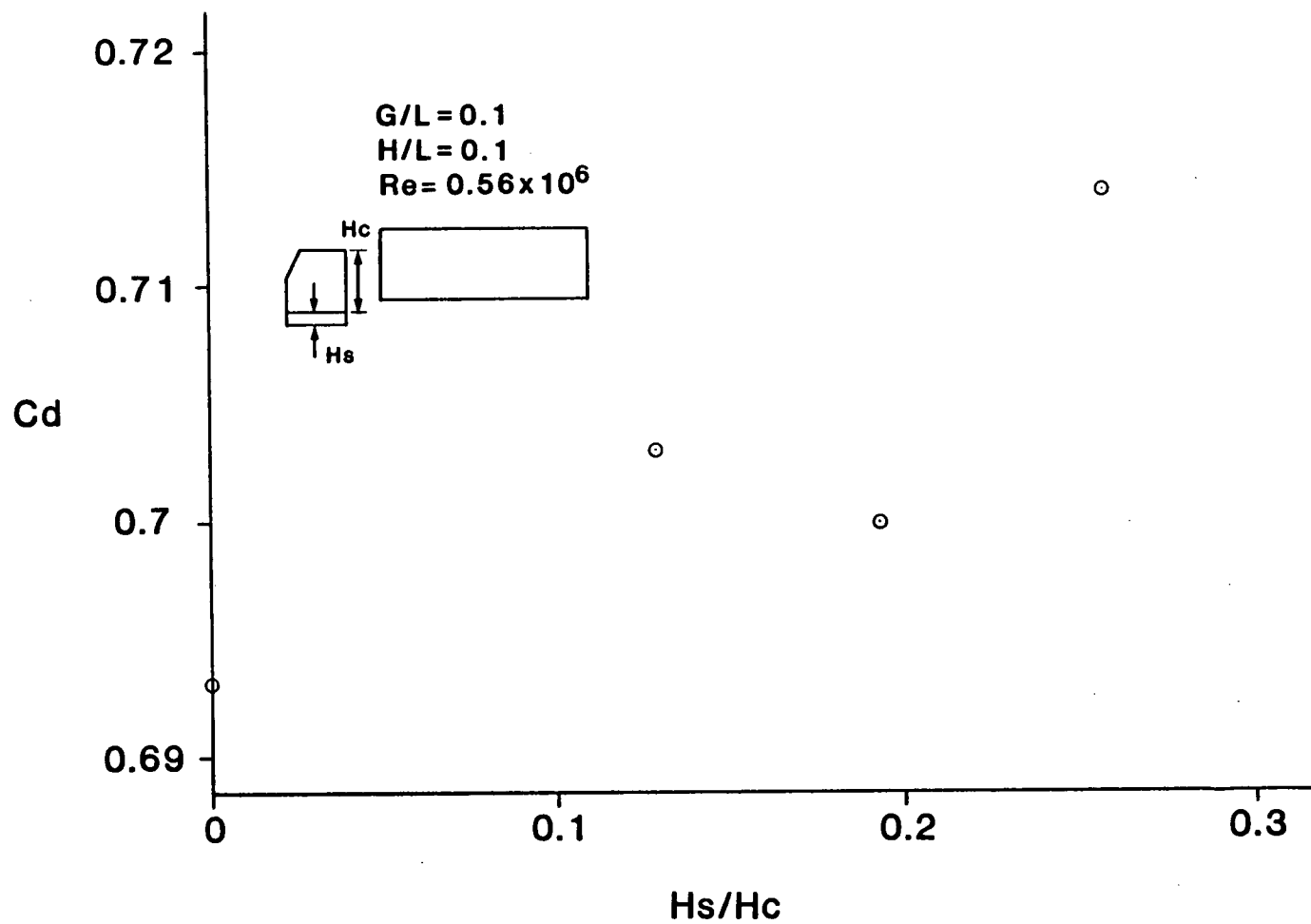


Figure 3-12. Drag coefficient versus non-dimensional tractor spoiler width H_s/H_c

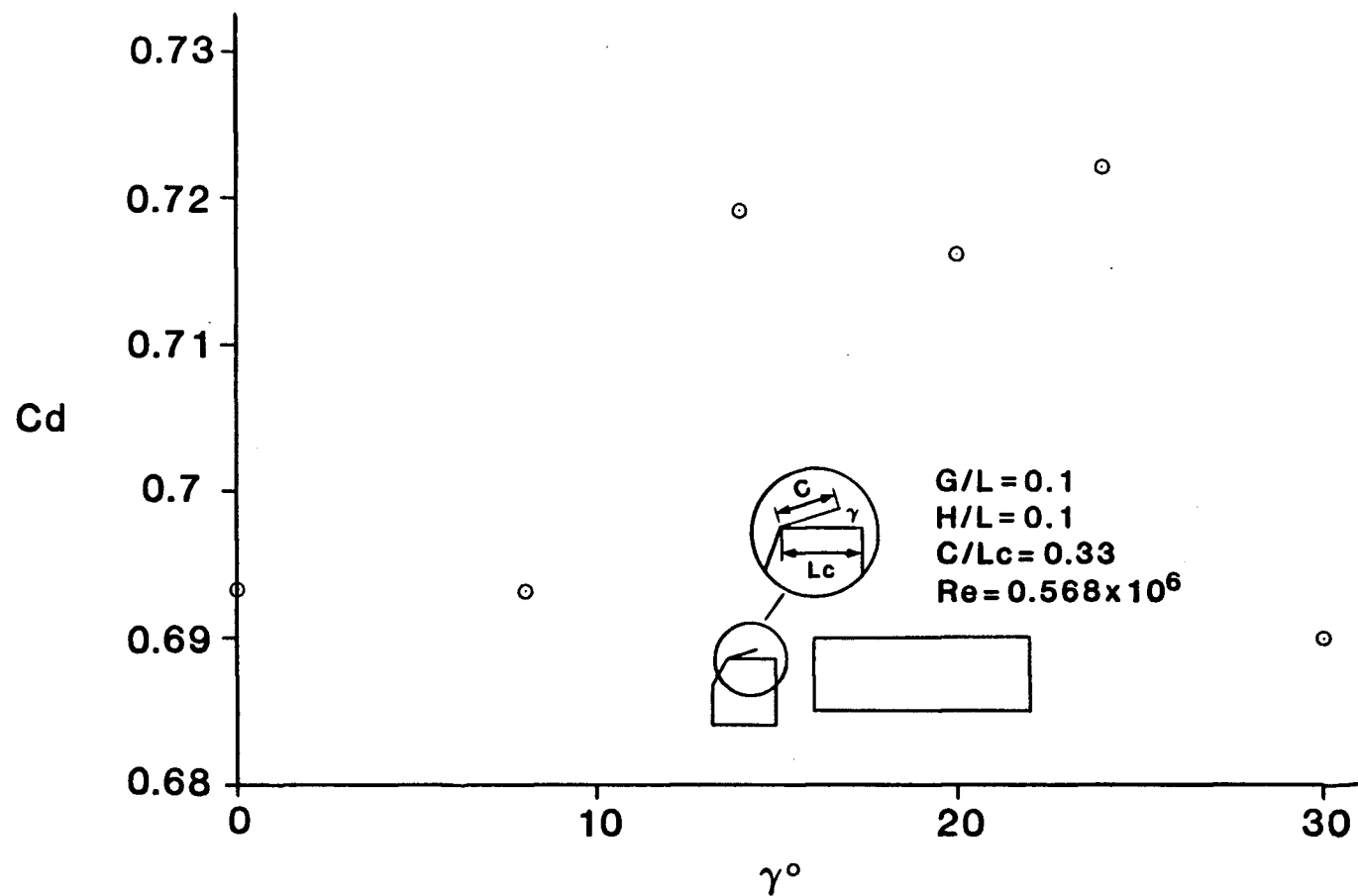


Figure 3-13. Variation of drag coefficient with tractor roof deflector angle γ for a given deflector length $C/L_c = 0.33$

= 0.5 at two Reynolds numbers; 0.545×10^6 and 0.623×10^6 . Note a very slight drag reduction at $\gamma = 30^\circ$ (Figure 3-13). On the other hand, Figure 3-14 shows a substantial decrease in C_d at $\gamma = 30^\circ$ for both Reynolds numbers tested. It is interesting to recognize that in this test, the deflector angle corresponding to a minimum drag (i.e., smooth flow reattachment at the trailer roof) is the same for both the Reynolds numbers.

3.3.3 Gap seals

Table 3-1 summarizes the results obtained using various combinations of gap-seals. As can be seen, all combinations had little or no beneficial effect on the drag.

3.4 Moving Surface Boundary Layer Control

Figure 3-15 shows drag coefficient versus non-dimensional surface velocity for the cylinder located at the top leading edge of the trailer. The Reynolds number was 0.55×10^6 . At zero velocity, the model had a lower drag than the one tested earlier. This is due to the rounded edges at the front and back of the tractor and trailer roofs (This modification, incidentally, works quite well, yielding a 12% reduction in drag.). The results with increasing cylinder velocity showed an initial increase in drag followed by a reduction at a velocity ratio of $V/U = 1.8$. Beyond this value, the drag increases again, although higher velocities ($V/U > 3$) would seem to be required to realize the full benefits of this approach to boundary layer control through moving surfaces [8]. Unfortunately, due to slippage of the o-ring, power capability of

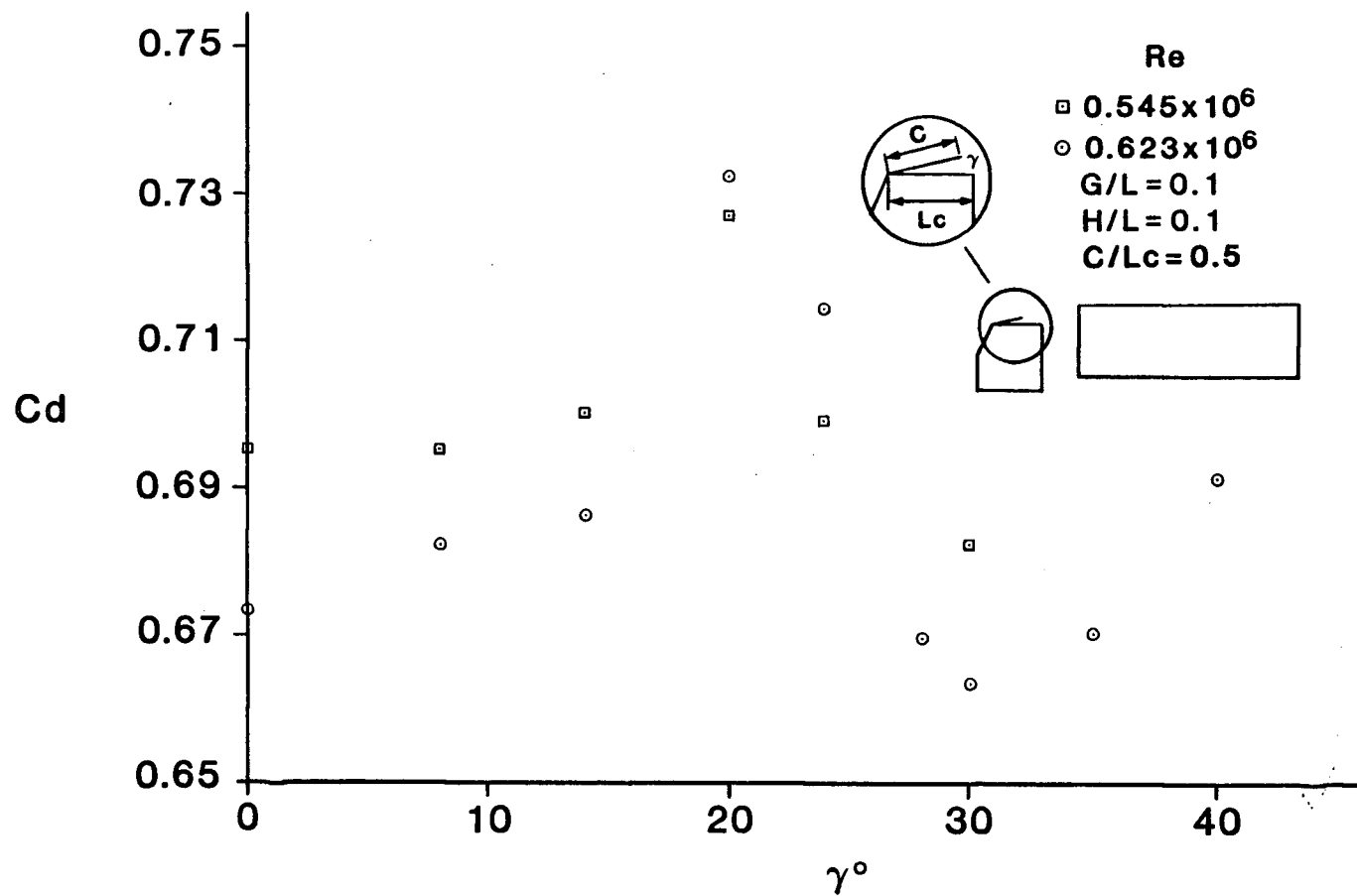


Figure 3-14. Variation of drag coefficient with tractor roof deflector angle γ for a given deflector length $C/L_c = 0.5$

Table 3-1

Drag coefficient for various gap sealing devices

Configuration	Drag Coefficient
No Seal	0.680
Top Only	0.680
Sides Only	0.690
Bottom Only	0.687
Top and Bottom	0.679
Top and Sides	0.687
Sides and Bottom	0.693
All Seals	0.705

$$Re = 0.6 \times 10^6$$

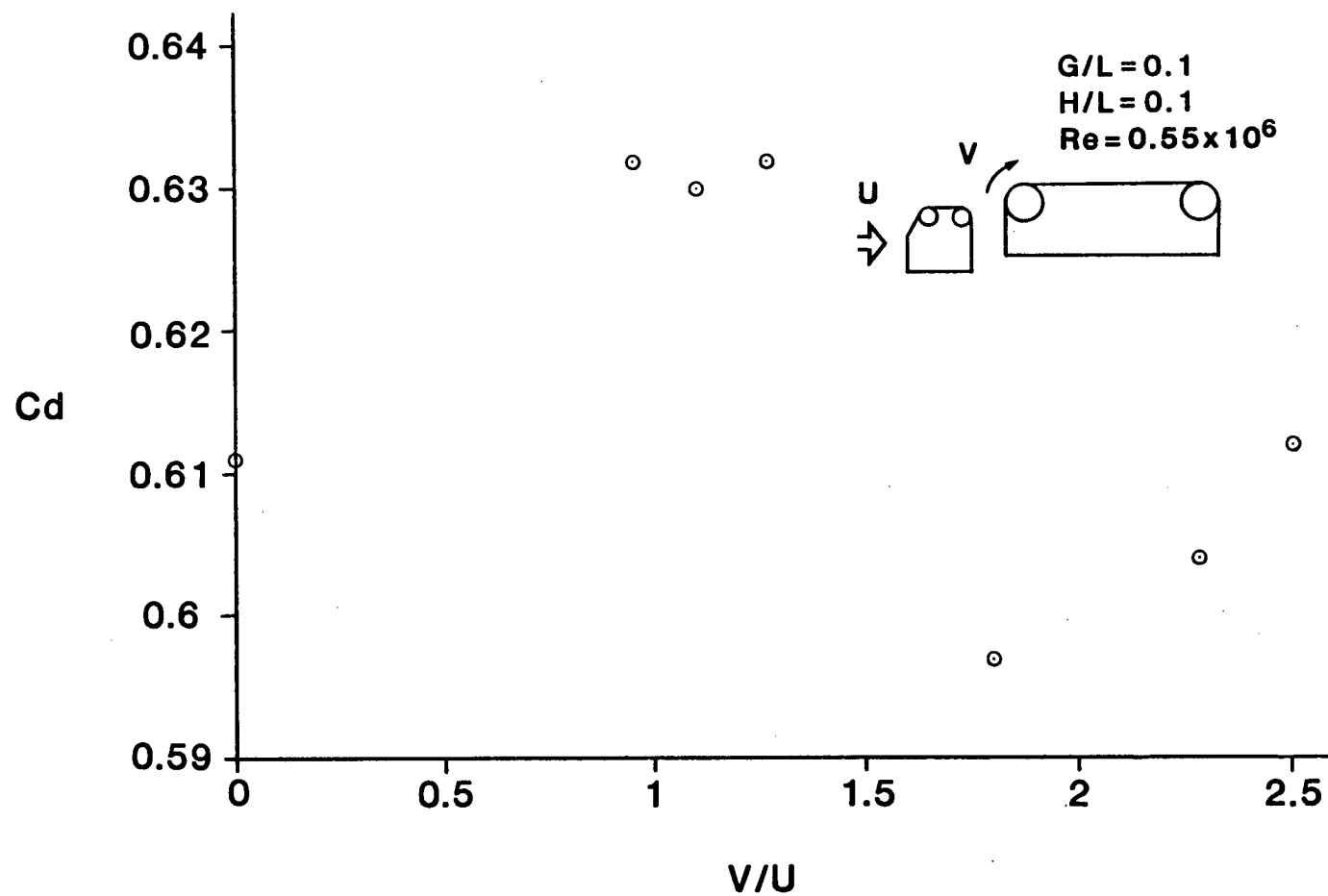


Figure 3-15. Effect of the trailer leading edge cylinder rotation on drag coefficient

the motor and space constraints it was not possible to attain higher cylinder rpm. Due to the extensive modifications required to the model and the large number of variables involved it was decided to assess the validity of the concept through a separate project.

For ease of comparison, Table 3-2 summarizes results of the entire test program.

Table 3-2

Summary of drag reductions with various configurations
and add-on devices

Configuration	Cd	Cd Reduction (%)
Conventional	0.71	-
Optimized (Base)	0.67 (= Cdo)	5.6
Base + 20° Back	0.64	9.9
Base + 5° Roof	0.60 (Cdo = 0.68)	16.9
Base + Roof Deflector	0.66	1.5*
Trailer Leading Edge Rotating Cylinder	0.597 (Cdo = .611)	2.3*

*These drag reductions are with respect to Cdo

4. CONCLUDING REMARKS

4.1 Conclusions

Based on the results and observations during the test program, the following general conclusions can be drawn:

- (i) Configuration changes have a greater effect on drag than add-on devices. With respect to the base configuration, a 5° backward sloping roof resulted in a 12% drag reduction while the tractor roof deflector resulted in a reduction of only 1.5%.
- (ii) Relatively minor configuration changes can result in large drag reductions. For example, a 2° backward sloping roof yields a 6% decrease in drag coefficient.
- (iii) Not all add-on devices have a beneficial effect and those that do are geometry dependent. For instance, addition of a roof deflector ($C/L_c = 0.5$) at 30° inclination resulted in a 1.5% reduction in drag coefficient while the same deflector at 20° inclination resulted in a 5% increase.
- (iv) The maximum drag reduction achieved through configuration changes and add-on devices is 16.9%.
- (v) Moving surface boundary layer control looks promising, however, its effectiveness needs to be verified through a carefully planned experiment.

4.2 Recommendations for Future Work

As with all preliminary studies, several areas are open to further study:

- (i) Because the devices and configuration changes would be used at highway speeds, tests should be performed at the corresponding Reynolds number (2×10^7 for 100 km/h). The use of wind tunnel facilities at the National Research Council should be explored to this end.
- (ii) Effectiveness of additional add-on devices such as gap splitter plates, trailer rear fairings and tractor roof deflectors of different geometries should be explored.
- (iii) Details should be added to the models to gauge their influence on the add-on devices and configuration changes.
- (iv) The tractor-trailer model should be modified to provide positive drive and higher speed to all four cylinders. This can be accomplished with more powerful motors transmitting power through belt, chain or gear drives. The boundary layer control should be tested with the cylinders operating individually and in various combinations over a range of surface velocity.

REFERENCES

- [1] Roshko, A. and Koenig, K., "Interaction Effects on the Drag of Bluff Bodies in Tandem," Proceedings of the Symposium on Aerodynamic Drag Mechanisms of Bluff Bodies and Road Vehicles, Ed. G. Sovran, T. Morel and W.T. Mason, Jr., Plenum Press, New York, 1978.
- [2] Ahmed, S.R. and Baumert, W., "The Structure of Wake Flow Behind Road Vehicles," Aerodynamics of Transportation, Ed. T. Morel and C. Dalton, ASME, New York, 1973.
- [3] Mair, W.A., "Drag-Reducing Techniques for Axi-Symmetric Bluff Bodies," Proceedings of the Symposium on Aerodynamic Drag Mechanisms of Bluff Bodies and Road Vehicles, Ed. G. Sovran, T. Morel and W.T. Mason, Jr., Plenum Press, New York, 1978.
- [4] Wong, H.Y., Cox, R.N. and Rajan, A., "Drag Reduction of Trailer-Tractor Configuration by Aerodynamic Means," Proceedings of the 4th Colloquium on Industrial Aerodynamics, Ed. C. Kramer and H.J. Gerhardt, Fotodruck Mainz, Aachen, 1980.
- [5] Mason, W.T., Jr. and Beebe, P.S., "The Drag Related Flow Field Characteristics of Trucks and Buses," Proceedings of the Symposium on Aerodynamic Drag Mechanisms of Bluff Bodies and Road Vehicles, Ed. G. Sovran, T. Morel and W.T. Mason, Jr., Plenum Press, New York, 1978.
- [6] "Truck and Bus Aerodynamics Investigated," Automotive Engineering, Vol. 88, No. 11, 1980, pp.50-57.
- [7] Rose, M.J., "Commercial Vehicle Fuel Economy - The Correlation Between Aerodynamic Drag and Fuel Consumption on a Typical Truck," Proceedings of the 4th Colloquium on Industrial Aerodynamics, Ed. C. Kramer and H.J. Gerhardt, Fotodruck Mainz, Aachen, 1980.
- [8] Modi, V.J., Swinton, P.G., McMillan, K., Lake, P., Mullins, D., and Akutsu, T., "Moving Surface Boundary layer Control for Aircraft Operation at High Incidence," Journal of Aircraft, AIAA, Vol. 18, No. 11, November 1981, pp.963-968.
- [9] Catalano, G.D., Viets, H. and Bougine, D., "Reduction of the Turbulent Wake of a Road Vehicle by use of Unsteady Vortex Shedding," AIAA 21st Aerospace Sciences Meeting, Reno, Nevada, USA, January 1983, paper No. AIAA-83-0427.